



Coupled carbon-water exchange of the Amazon rain forest, II. Comparison of predicted and observed seasonal exchange of energy, CO₂, isoprene and ozone at a remote site in Rondônia

E. Simon, F. X. Meixner, U. Rummel, L. Ganzeveld, C. Ammann, J. Kesselmeier

► To cite this version:

E. Simon, F. X. Meixner, U. Rummel, L. Ganzeveld, C. Ammann, et al.. Coupled carbon-water exchange of the Amazon rain forest, II. Comparison of predicted and observed seasonal exchange of energy, CO₂, isoprene and ozone at a remote site in Rondônia. *Biogeosciences*, 2005, 2 (3), pp.255-275. hal-00297525

HAL Id: hal-00297525

<https://hal.science/hal-00297525>

Submitted on 18 Jun 2008

HAL is a multi-disciplinary open access archive for the deposit and dissemination of scientific research documents, whether they are published or not. The documents may come from teaching and research institutions in France or abroad, or from public or private research centers.

L'archive ouverte pluridisciplinaire **HAL**, est destinée au dépôt et à la diffusion de documents scientifiques de niveau recherche, publiés ou non, émanant des établissements d'enseignement et de recherche français ou étrangers, des laboratoires publics ou privés.

Coupled carbon-water exchange of the Amazon rain forest, II. Comparison of predicted and observed seasonal exchange of energy, CO₂, isoprene and ozone at a remote site in Rondônia

E. Simon¹, F. X. Meixner¹, U. Rummel², L. Ganzeveld³, C. Ammann⁴, and J. Kesselmeier¹

¹Biogeochemistry Dept., Max Planck Institute for Chemistry, Mainz, Germany

²Meteorologisches Observatorium Lindenberg, Deutscher Wetterdienst, Germany

³Atmospheric Chemistry Dept., Max Planck Institute for Chemistry, Mainz, Germany

⁴Swiss Federal Research Station for Agroecology and Agriculture, Zürich, Switzerland

Received: 24 February 2005 – Published in Biogeosciences Discussions: 7 April 2005

Revised: 15 August 2005 – Accepted: 28 September 2005 – Published: 18 October 2005

Abstract. A one-dimensional multi-layer scheme describing the coupled exchange of energy and CO₂, the emission of isoprene and the dry deposition of ozone is applied to a rain forest canopy in southwest Amazonia. The model was constrained using mean diel cycles of micrometeorological quantities observed during two periods in the wet and dry season 1999. Calculated net fluxes and concentration profiles for both seasonal periods are compared to observations made at two nearby towers.

The modeled day- and nighttime thermal stratification of the canopy layer is consistent with observations in dense canopies. The observed and modeled net fluxes above and H₂O and CO₂ concentration profiles within the canopy show a good agreement. The predicted net carbon sink decreases from 2.5 t C ha⁻¹ yr⁻¹ for wet season conditions to 1 t C ha⁻¹ yr⁻¹ for dry season conditions, whereas observed and modeled midday Bowen ratio increases from 0.5 to 0.8. The evaluation results confirmed a seasonal variability of leaf physiological parameters, as already suggested in a companion study. The calculated midday canopy net flux of isoprene increased from 7.1 mg C m⁻² h⁻¹ during the wet season to 11.4 mg C m⁻² h⁻¹ during the late dry season. Applying a constant emission capacity in all canopy layers, resulted in a disagreement between observed and simulated profiles of isoprene concentrations, suggesting a smaller emission capacity of shade adapted leaves and deposition to the soil or leaf surfaces. Assuming a strong light acclimation of emission capacity, equivalent to a 66% reduction of the standard emission factor for leaves in the lower canopy, resulted in a better agreement of observed and modeled concentration profiles and a 30% reduction of the canopy net flux compared to model calculations with a constant emis-

sion factor. The mean calculated ozone flux for dry season conditions at noontime was $\approx 12 \text{ nmol m}^{-2} \text{ s}^{-1}$, agreeing well with observed values. The corresponding deposition velocity increased from 0.8 cm s⁻¹ to $> 1.6 \text{ cm s}^{-1}$ in the wet season, which can not be explained by increased stomatal uptake. Considering reasonable physiological changes in stomatal regulation, the modeled value was not larger than 1.05 cm s⁻¹. Instead, the observed fluxes could be explained with the model by decreasing the cuticular resistance to ozone deposition from 5000 to 1000 s m⁻¹.

1 Introduction

Within the last decade, detailed biosphere-atmosphere models have been developed to describe the exchange of energy and important atmospheric trace gases like CO₂, ozone and isoprene between the terrestrial vegetation and the lower atmosphere (Sellers et al., 1992; Leuning et al., 1995; Baldocchi and Meyers, 1998; Baldocchi et al., 1999). These models integrate knowledge from different scientific disciplines and may serve as helpful tools in geophysical research: in prognostic applications, they can be used to study the feedback between atmospheric and biophysical processes (such as the effect of CO₂ fertilization) and diagnostically, they can be used as a substitution and completion of costly field measurements.

In a companion paper, Simon et al. (2005a) describe a one-dimensional multilayer canopy model of coupled carbon-water exchange. This scheme includes detailed descriptions of ecophysiological exchange processes at the leaf scale, which are connected to the canopy scale by a Lagrangian dispersion model of vertical turbulent transport. Commonly, this model type is referred to as the “CANVEG” scheme,

Correspondence to: E. Simon
(simon@mpch-mainz.mpg.de)

originally invented by Baldocchi (1992) and Baldocchi and Meyers (1998). We adapted the CANVEG scheme for application to the Amazon rain forest. By using informations and data pools from intensive field campaigns, a generic characterization and parameterization of biophysical properties of the predominant vegetation type within the Amazon basin is given. In summary, the results presented in the companion paper include a characterization of mean canopy structure, the distribution of photosynthetic capacity and a normalized profile of horizontal wind speed. The subroutines to calculate the canopy radiation field and soil surface exchange as well as leaf photosynthesis and stomatal conductance, considering wet and dry season conditions, are evaluated using scale appropriate data. Finally, the sensitivity of modeled net fluxes to key parameter uncertainties is investigated and the uncertainty range of leaf physiological parameters is derived. The parameterization of the Lagrangian dispersion sub-model is discussed and evaluated in detail in a further study (Simon et al., 2005b).

In the present study, the parameterized model is applied to a remote site in Rondônia, Sout-West Brazil. Calculated net fluxes and vertical scalar profiles of H_2O , CO_2 , isoprene and ozone are compared to measurements made at two nearby micrometeorological towers during the late wet and late dry season 1999. The model is constrained using observed surface-layer meteorology and soil moisture status and soil temperature measured just below the soil surface. The following questions are addressed:

1. *Concept validation:* Are the environmental boundary-conditions in steady-state or does the coupling of surface exchange and vertical dispersion result in numerical instabilities of the modeled canopy temperature and H_2O and CO_2 concentrations?
2. *Model evaluation:* Is the model predicted thermal stratification of the canopy consistent with observations? How well do the fluxes and concentration profiles of CO_2 , H_2O , isoprene and O_3 predicted by the model agree with observations?
3. *Diagnostic model application:* To what extent does the model explain the observed variabilities of net fluxes and concentration profiles and how does the model contribute to our understanding of the processes which are involved in the exchange of important atmospheric trace gases?

Topic (1) is related to basic model assumptions. It has to be shown, that the interactive coupling of surface exchange and vertical mixing does not result in unstable or unrealistic numerical solutions, due to unsteady environmental conditions. This might occur if, for example, the air temperature or CO_2 concentration of a single canopy layer increases with every iteration step of surface exchange because the calculated vertical mixing rate is too slow. Topic (2) mainly in-

cludes a comparison of model results and observations. Measurements of leaf temperature and temperatures of the surrounding canopy air have not been available for direct evaluation. However, the calculated thermal stratification of the canopy may serve as a good indicator of model consistency. In the real world, the lower part of dense canopies often shows a typical diel pattern, which is the reverse compared to the atmospheric boundary-layer above (Jacobs et al., 1994; Bosveld et al., 1999, specifically for Amazon rain forest see Kruijt et al., 2000; Simon et al., 2005b). For further validation, direct eddy covariance fluxes of sensible heat, latent heat, CO_2 and O_3 measured above the canopy are used. Furthermore, the reliability of model results is advanced by including a comparison of measured and calculated scalar profiles of CO_2 , H_2O , isoprene and O_3 . This is very meaningful because the predicted fluxes may be in agreement with the measurements while the predicted concentrations profiles are not very realistic (as an example see Baldocchi, 1992). By using different data sets for model parameterization, application and evaluation (e.g. enclosure measurements at the leaf level in the companion paper, in-canopy concentration profiles and canopy net fluxes at the canopy level in the present study) a profound and complementary evaluation of our current knowledge on canopy processes is performed. (3) In general, the variability of energy and trace gas exchange is imposed by short- and longterm frequencies, i.e. the diel and annual solar cycles, respectively. We assessed the diel variabilities by analyzing mean diel cycles of net fluxes and typical day- and nighttime vertical concentration profiles. The longterm variability is characterized mainly by periods of high and low rainfall. Several studies on carbon and energy exchange of the Amazon rain forest have reported a strong seasonal variability of the canopy net fluxes of CO_2 and energy (Malhi et al., 1998; Williams et al., 1998; Andreae et al., 2002; Carswell et al., 2002; Malhi et al., 2002) and discuss whether the observed seasonality is triggered by ecophysiological (stomatal conductance, photosynthesis) or structural (LAI) factors.

In the companion paper (Simon et al., 2005a), it has been shown that the structural variability, as observed at different sites in Amazonia, causes relatively small changes in the calculated net fluxes. In contrast, the model is very sensitive to the choice of ecophysiological parameters which probably show systematic variations for wet and dry season conditions (see Malhi et al., 1998; Kuhn et al., 2004; Simon et al., 2005a). Therefore, we included a seasonal comparison of the observed and calculated diel cycles of canopy net fluxes for three different model parameterizations: In addition to a mean parameterization (1), leaf physiological parameters are modified within their uncertainty range, resulting in higher stomatal conductance rates for wet season conditions (2) and lower photosynthesis rates for dry season conditions (3, see Simon et al., 2005a).

Furthermore, current isoprene emission and ozone deposition algorithms have been integrated into the model and the

predicted fluxes and scalar profiles of these tracers are evaluated and discussed as well.

2 Materials and methods

2.1 Site description and field data

The modified CANVEG scheme is applied to a primary tropical rain forest in Rondônia (Reserva Jaru, see Simon et al., 2005a). This site was the main forest research site of LBA-EUSTACH¹ and is described in detail by Andreae et al. (2002). Measurements have been performed simultaneously at two towers, RBJ-A and RBJ-B, during two intensive field campaigns, hereafter referred to as EUST-I and EUST-II, respectively, coinciding with the late wet (April–May) and late dry season (September–October) in 1999. At RBJ-B, eddy covariance fluxes of CO₂, H₂O, and sensible heat were measured at 62 m above the ground, whereas concentration profiles of CO₂ and H₂O were sampled at 62.7, 45, 35, 25, 2.7 and 0.05 m (Andreae et al., 2002). At RBJ-A, eddy covariance fluxes of CO₂, H₂O, sensible heat and ozone were measured at 53 m above the ground, concentrations profiles of CO₂, H₂O, and ozone were sampled at 51.7, 42.2, 31.3, 20.5, 11.3, 4, 1 and 0.3 m (Rummel, 2005; Andreae et al., 2002). The forcing data (surface-layer meteorology above the canopy i.e. relative humidity, air temperature, barometric pressure, incoming global radiation, mean horizontal wind speed, standard deviation of vertical wind speed, background CO₂ and ozone concentration; soil moisture status and temperature at −0.05 m) has been measured at RBJ-A. Additionally, measurements of isoprene concentrations were made simultaneously at 1, 25, 45 and 52 m height during a short period at the end of the dry season, as described in detail by Kesselmeier et al. (2002). Most of the data have been published recently (a comprehensive overview is given by Andreae et al., 2002). The time series of the micrometeorological data, net fluxes and scalar profiles (except isoprene), available with a time resolution of 30 min, have been averaged to hourly means of two diel cycles for wet (EUST-I) and dry season (EUST-II) conditions, respectively. Note, that the time given in all graphs indicates interval start (e.g. 8 h represents the time interval from 8–9 h).

The net fluxes of sensible heat, H₂O, CO₂, and ozone measured above the canopy have to be corrected by the canopy volume storage flux for a direct comparison with the model predicted “instantaneous” fluxes. The storage fluxes for CO₂ and ozone are calculated according to Grace et al. (1995) from the temporal evolution of the diurnally averaged vertical concentration profiles. The empirical relationship of Moore and Fisch (1986), evaluated for RBJ-A by Rummel (2005), was applied to determine the energy storage

Table 1. Seasonal comparison of climatic variables observed at the Jaru site in Rondônia (mean values if not specified).

Parameter	EUST-I	EUST-II
Precipitation ^{*,a,c} (mm)	950	550
Radiation ^c (MJ m ^{−2} d ^{−1})	16.7	19.9
Temperature ^c (°C)	24.3	25.7
Humidity ^c (g kg ^{−1})	2.5	5.2
Soil water content ^d (–)	0.25	0.15
Ozone concentration ^{†,a–c} (ppb)	10	40
Isoprene concentration ^{†,b} (ppb)	4	12
Aerosol particles ^a (cm ^{−3})	450±320	6200±4800
NO _x concentration ^{†,a–c} (ppb)	0.08	0.44

^a Andreae et al. (2002), ^b Kesselmeier et al. (2002),

^c Rummel (2005), ^d Gut et al. (2002b)

* total sum from Dec’98 to May’99 and Jun–Nov’99

† typical midday values above the canopy

terms, using the temperature and humidity observed above the canopy.

2.2 Meteorological overview

The mean diel cycles of micrometeorological forcing parameters observed at RBJ-A during EUST-I and EUST-II are shown in Fig. 1. A seasonal comparison of additional climatic variables is listed in Table 1. Global radiation reaches maximum values of 400–900 W m^{−2} around noon time with distinctly larger values during the late dry season. The CO₂ concentration shows a strong diurnal variability with maximum and minimum values between 460 and 365 ppm during night- (4–6 h) and daytime (15–16 h), respectively. The wet season daytime minimum values are slightly lower (361 ppm) compared to the dry season (367 ppm). Furthermore, relative humidity during EUST-I was larger and incoming radiation and temperature were lower compared to the dry season. Mean daytime maximum temperature and diurnal amplitude was 3°C higher during the dry season, coinciding with a decrease of relative humidity. The noon time values decreased from 72% to 60%, whereas the specific humidity was twice as high for dry compared to wet season conditions, respectively. The soil temperature was only slightly higher during the dry season whereas the mean soil water content decreased approximately from 25 to 15%. The wet-to-dry seasonal changes of humidity, temperature, and radiation were accompanied by the occurrence of large-scale biomass burning leading to a strong increase in aerosol particles and ozone concentrations (see Table 1). In contrast, the mean diel cycles of horizontal wind speed (Fig. 1c, d) and other turbulent quantities are very similar for both seasonal periods.

¹Large-scale Biosphere-atmosphere experiment in Amazonia – European Studies on trace gases and Atmospheric CHemistry

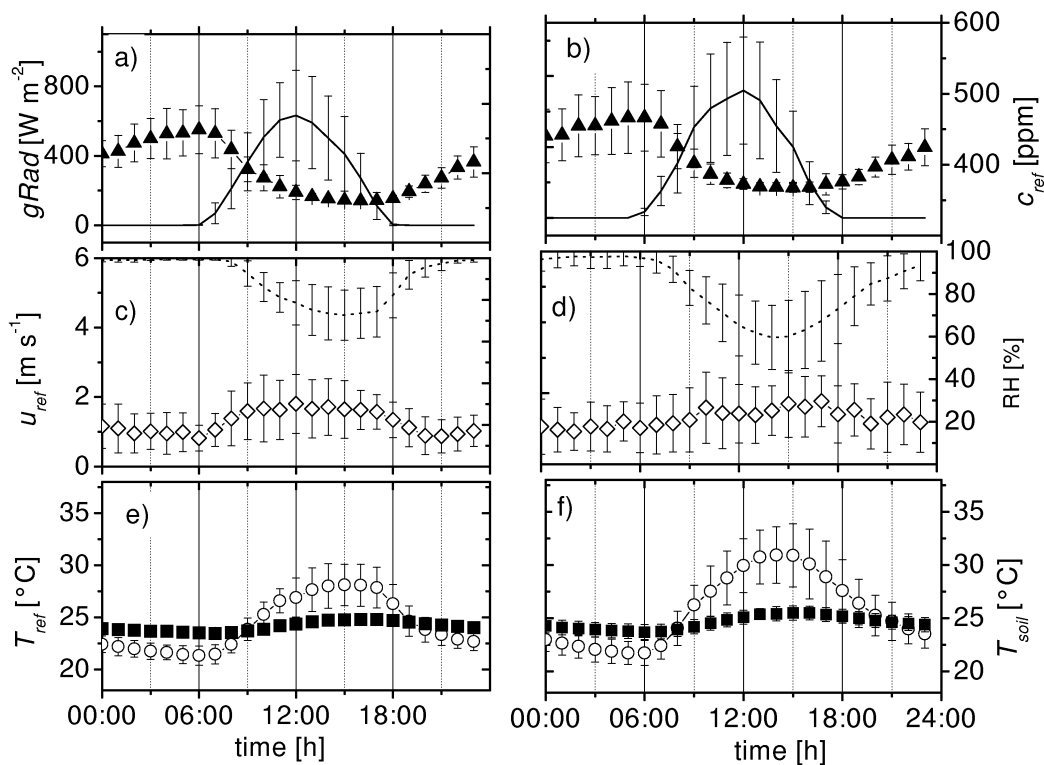


Fig. 1. Means and standard deviations of micrometeorological quantities during EUST-I and EUST-II at the Jaru site in Rondônia in 1999. **(a, b)** Incoming global radiation ($gRad$, solid line) and CO_2 concentration (c_{ref} , filled triangles). **(c, d)** Mean horizontal wind speed (u_{ref} , open diamonds) and relative humidity (RH , dotted line). **(e, f)** Air (T_{ref} , open circles) and soil temperature (T_{soil} , closed squares). All quantities except T_{soil} (-0.05 cm) were measured above the canopy at $z_{ref}=53$ m above the ground.

Table 2. Uncertainty range of leaf model parameters inferred in Simon et al. (2005a) and applied as the reference (REF), wet (EUST-I) and dry season (EUST-II) parameterization to assess the control on observed seasonality (a_N represents the empirical coefficient relating net assimilation to stomatal conductance, θ the shape parameter of the hyperbolic light response of photosynthesis).

Model parameter	REF	EUST-I	EUST-II
A_n - g_s -relationship a_N (–)	10	15	10
Light use efficiency α (–)	0.15	0.15	0.13
Shape parameter θ (–)	0.9	0.9	0.85

2.3 Model setup

The parameterization of the CANVEG scheme and the Lagrangian transport sub-model are described in detail in Simon et al. (2005a) and Simon et al. (2005b), respectively. A bi-modal leaf area density distribution with $LAI=6$ and a mean canopy height $h_c=40$ m is applied. A number of 8 equidistant canopy layers of 5 m depth has been selected

with a surface layer of 13 m depth above h_c and below $z_{ref}=53$ m. Modeled canopy albedo is optimized by scaling leaf optical parameters. Soil respiration is calculated applying the observed reference value of $3.3\ \mu mol\ m^{-2}\ s^{-1}$ at $25^{\circ}C$ and an activation energy of $60\ kJ\ mol^{-1}$. The light acclimation parameter for leaf photosynthesis is set to $k_N=0.2$ with a maximum carboxylation rate of $50\ \mu mol\ m^{-2}\ s^{-1}$ at the canopy top. The temperature dependence of leaf photosynthesis is calculated using optimized values for the activation energy of electron transport and entropy ($H_{v,J}=108$ and $S_J=0.66\ kJ\ mol^{-1}$, respectively), resulting in a lower temperature optimum of the light reaction of photosynthesis compared to the recommended parameterization. For details see Simon et al. (2005a).

The question whether the observed variability of canopy net fluxes (see Sect. 1) may be driven by changing leaf physiology, is addressed by modifying three leaf model parameters (see Table 2): A reference parameterization using the same values for both seasonal periods (1), a parameterization predicting higher stomatal conductance rates (g_s) for EUST-I by increasing the parameter correlating g_s with net assimilation A_n (2, see also Lloyd et al., 1995a), and a third

parameterization predicting lower A_n for EUST-II by decreasing the quantum yield of electron transport (α , the light-use efficiency and initial slope of light response) and the shape parameter of the hyperbolic light response function (θ).

For clarification, please note that the different parameterizations applied for wet and dry season conditions are, up to now, not explicitly proofed by measurements. However, the seasonal variability of leaf trace gas exchange is evident (see Sect. 1). By comparing the different model results with observations, we can test whether model parameter uncertainties are necessary or sufficient to explain the observed seasonal variability of canopy fluxes. Subsequently, appropriate experiments have to be designed in the future, to reduce the model uncertainty by reducing model parameter uncertainty.

Isoprene emission at the leaf scale is calculated according to Guenther et al. (1993). A standard emission factor of $24 \mu\text{g C g}^{-1} \text{h}^{-1}$ and a specific leaf dry weight of 125 g m^{-2} (Guenther et al., 1995) is applied for leaves at the canopy top. Note, that this parameterization is equivalent to an assumed fraction of 30% isoprene emitting species, each having a standard emission factor of $80 \mu\text{g C g}^{-1} \text{h}^{-1}$ at the canopy top (see also Harley et al., 2004). Several studies have demonstrated that the emission capacity of single leaves for isoprene and monoterpenes is influenced by leaf acclimation to the light and temperature environment (Sharkey et al., 1991; Harley et al., 1994; Hanson and Sharkey, 2001a,b; Staudt et al., 2003). For 20 tree species of a tropical rain forest in Costa Rica, Geron et al. (2002) compared the emission capacity of sun-exposed foliage to leaves growing in low-light environment. On average, the emission capacity of shade adapted leaves were reduced by two third compared to sun-exposed leaves. Consequently, a vertical scaling of the isoprene standard emission factor $E_{V0}^m(z)$ was performed assuming a linear dependence on canopy position (accumulated leaf area Λ_z). Given LAI=6 and the observed 66% reduction of E_{V0}^m for leaves close to the ground predicts

$$E_{V0}^m(\Lambda_z) = E_{V0}^m(\Lambda_{hc}) - 2.7\Lambda_z \quad (1)$$

which results, for example, in a standard emission factor of $8 \mu\text{g C g}^{-1} \text{h}^{-1}$ close to the ground (see also Guenther et al., 1999).

Ozone uptake is calculated by applying the concept of dry deposition, assuming that chemical sources and sinks for ozone production and consumption within the canopy are negligible. This simplification will be discussed later. Generally, the dry deposition velocity is given by

$$v_{d,x} = \frac{F_x}{c_x(z_{\text{ref}})}, \quad (2)$$

representing the kinematic flux F_x of a tracer x , normalized by the tracer concentration c_x at z_{ref} above the canopy. Eq. (2) is applicable for trace gases which are deposited to leaf and soil surfaces, whereby the trace gas concentration

inside the leaf (and soil) is assumed to be zero (see also Baldocchi et al., 1987; Ganzeveld and Lelieveld, 1995).

In contrast to bulk models that treat the canopy as a big leaf, multilayer models can resolve deposition at a much smaller scale and distinguish explicitly between deposition that is controlled by transport, and deposition that is controlled by leaf physiology and soil activity. Firstly, v_d is decomposed into the uptake by the soil and the parallel uptake in all canopy layers $v_{d,i}$, $i=0,\dots,m$ according to

$$v_d = v_{d,\text{soil}} + \sum_{i=0}^m v_{d,i}. \quad (3)$$

Secondly, $v_{d,i}$ and $v_{d,\text{soil}}$ are expressed as series (i.e. sums) of resistances according to

$$\frac{v_{d,i}}{\Lambda_i} = \frac{1}{r_a(z_i) + r_{\text{leaf},\text{O}_3}} \quad (4)$$

$$v_{d,\text{soil}} = \frac{1}{r_a(z=0) + r_{\text{soil},\text{O}_3}}, \quad (5)$$

where Λ_i represents the leaf surface in layer i . Deposition limited by transport is represented by $r_a(z_i)$, the aerodynamic resistance to transport from z_{ref} to z_i , which is equivalent to the integrated dispersion coefficient between these heights (see Simon et al., 2005b). Deposition limited by leaf and soil processes are represented by $r_{\text{leaf},\text{O}_3}$ and $r_{\text{soil},\text{O}_3}$, respectively. According to Baldocchi et al. (1987), $r_{\text{leaf},\text{O}_3}$ for hypo-stomatous leaves can be divided into a stomatal and cuticular pathway according to

$$\frac{1}{r_{\text{leaf},\text{O}_3}} = \frac{1}{r_{b,\text{O}_3} + r_{s,\text{O}_3} + r_{m,\text{O}_3}} + \frac{2}{r_{b,\text{O}_3} + r_{\text{cut},\text{O}_3}}. \quad (6)$$

The leaf boundary-layer (r_b) and stomatal (r_s) resistance are derived from the conductances for water vapor using the ratio's of molecular diffusivities (Massman, 1998). The intercellular ozone concentration and consequently the mesophyll resistance r_{m,O_3} are assumed to be zero (Chameides, 1989; Wesely, 1989; Neubert et al., 1993; Gut et al., 2002a). The factor of two on the right hand side of Eq. (6) indicates, that cuticular exchange occurs at both leaf sides. Although the cuticular resistance ($r_{\text{cut},\text{O}_3}$) is relatively large (Gut et al., 2002a), the significance of this pathway to total deposition has been shown recently by Rummel (2005), estimating a value of $4000\text{--}5000 \text{ s m}^{-1}$. The resistance to soil deposition $r_{\text{soil},\text{O}_3}$ was estimated as 188 s m^{-1} from dynamic chamber measurements by Gut et al. (2002a). Adding this value to the bulk soil surface resistance (transport from the mean height of the lowest canopy layer at 2.5 m to the soil surface $1/g_{\text{soil}} \approx 500 \text{ s m}^{-1}$, see companion paper) results in a total soil resistance of $r_{\text{soil},\text{O}_3} \approx 700 \text{ s m}^{-1}$.

The assumption, that chemical reactions of ozone within the canopy are negligible for the calculation of the ozone budget is supported by experimental results of several LBA-EUSTACH studies: In the case of NO_x chemistry, Meixner et al. (2002) and Rummel (2005) compared the chemical, biological and transport timescales of relevant reactions of

the NO-NO₂-O₃ triad (see Bakwin et al., 1990; Jacob and Wofsy, 1990; Chameides and Lodge, 1992; Yienger and Levy, 1995; Ganzeveld et al., 2002) at our site (see also Gut et al., 2002a,b). Above the canopy, chemical reactions are much slower compared to turbulent exchange and can be neglected. At 11 m in the lower canopy, turbulent transport is still efficient, and the biological uptake of ozone is one order of magnitude faster than ozone chemistry. Below 10 m, the photolysis rate is too small for ozone production by NO₂ oxidation, so that only ozone destruction by NO has to be considered. In this case, the chemical, biological and transport timescales are in the same order of magnitude. However, this is only relevant for the NO budget: The maximum chemical loss term of ozone due to reduction by NO is equivalent to the total soil NO flux, which is at least one order of magnitude lower ($<0.7 \text{ nmol m}^{-2} \text{ s}^{-1}$) than the mean observed ozone fluxes ($>3 \text{ nmol m}^{-2} \text{ s}^{-1}$ Gut et al., 2002b; Rummel, 2005).

A second potential ozone destruction mechanism involves chemical reactions with highly reactive gaseous organic compounds. Recent studies on a ponderosa pine plantation in the Sierra Nevada Mountains, California have proven evidence, that ozone destruction by highly reactive biogenic volatile organic compounds, hereafter referred to as BVOC, might contribute up to 50% to the total ozone flux (Kurpius and Goldstein, 2003; Goldstein et al., 2004; Holzinger et al., 2005). Due to their high reactivity these compounds are unfortunately experimentally hard to determine. However, smaller emissions and much lower concentrations of those BVOC's that are actually detectable by gas chromatography/mass spectrometry have been observed within and above the canopy at our site (Kesselmeier et al., 2002; Greenberg et al., 2004) compared to the ponderosa pine site. Furthermore, the composition of BVOC's in tropical rain forests is generally dominated by isoprene and differs significantly from the BVOC composition in coniferous forests. This potential contribution of chemical reactions to the ozone fluxes is discussed in more detail in Sect. 3.4.

3 Results and discussion

3.1 Canopy thermal stratification

The assumption of steady-state environmental conditions implies that leaf surface exchange and vertical mixing are in balance. This assumption is usually fulfilled when meteorological quantities change slowly. However, for short periods the environmental conditions may change rapidly, e.g. due to rainfall or large scale turbulence structures. Therefore, only time-averaged micrometeorological quantities were considered and periods with rain were rejected. The day- and nighttime transition periods at sunrise and sunset represent further situations, where micrometeorological conditions are unsteady. Probably the most appropriate indicators for con-

ditions where the steady-state assumption is not fulfilled are the temperature differences between the leaf surface and the ambient air within and above the canopy ($T_s - T_a$, $T_a - T_{\text{ref}}$, respectively). Therefore, the modeled canopy thermal stratification has been analyzed in detail.

Figure 2 shows the diel cycle of the calculated differences between the mean foliage temperature, the ambient air within and the surface layer above the canopy (for EUST-I) and the number of model iterations required for model conversion (EUST-I and EUST-II). One iteration includes the calculation of the vertical source/sink distribution of energy and CO₂ and the resulting change in the scalar profiles. Conversion is reached when the mean change of the temperature profile for a new iteration is less than 0.01 K (see Simon et al., 2005a). The mean foliage and ambient air temperatures ($T_{s,av}$, $T_{a,av}$) are calculated as the surface (leaf) area and layer volume weighted average of the vertical profiles of T_s and T_a , respectively. T_s is calculated as the sunlit and shaded leaf fraction weighted surface temperature. During daytime, the foliage and canopy air are heated by solar radiation and the model predicts $T_{s,av} - T_{a,av} \approx 1.5^\circ\text{C}$ and $T_{a,av} - T_{\text{ref}} \approx 0.5^\circ\text{C}$ at noontime. During sunset, the foliage cools off, the radiation budget of the canopy changes its sign and steady-state calculations fail to converge. Obviously, model assumptions are violated under these circumstances since the micrometeorological conditions are changing towards a new state. This highlights interesting interactions between the vegetation layer, the soil surface below and the atmospheric boundary-layer above. For nighttime conditions, model calculations are consistent again predicting negative gradients $T_{s,av} - T_{a,av} \approx T_{a,av} - T_{\text{ref}} \approx -0.4^\circ\text{C}$. As shown in Fig. 2b, 2–10 iterations are required for conversion for daytime conditions, correlating negatively with ΔT (Fig. 2a). For nighttime conditions, a constant number of 4 iterations is required.

Stable model solutions for steady-state environmental conditions are shown in more detail in Fig. 3. For daytime conditions, the model predicts large temperature gradients across the leaf boundary layer ($T_s - T_a$) and sunlit and shaded leaf surfaces. This is very important for physiological processes, which imply usually a non-linear temperature response. Assuming a typical Q_{10} -value of 2, a temperature increase of 5°C would increase the physiological response by 50%.

As observed in real canopies, foliage temperature reaches maximum values in the upper canopy, where most of the irradiance is absorbed. At $0.75 h_c$, the mean leaf temperature is mainly determined by the surface temperature of sunlit leaves, which is $2\text{--}4^\circ\text{C}$ higher compared to shaded leaves. Close to the ground, $T_s - T_a$ becomes small. To assess the sensitivity of these calculations to leaf physiological parameters, the parameter modifications listed in Table 2 have been applied in additional simulations (represented as error bars shown in Fig. 3). Increasing stomatal conductance (by increasing a_N) has a cooling effect on T_s resulting in a decrease of $0.3\text{--}1.2^\circ\text{C}$ for EUST-I. Decreasing

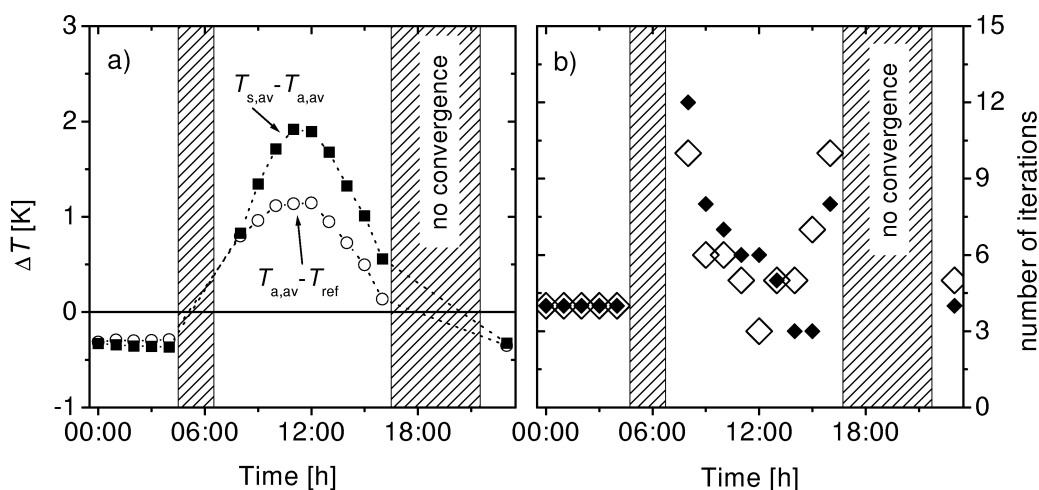


Fig. 2. (a) Diel cycle of the temperature differences between the foliage and the ambient air ($T_{s,av} - T_{a,av}$, solid squares) and between the ambient air and the surface layer ($T_{a,av} - T_{ref}$, circles), calculated for EUST-I (Fig. 1a, c, e). (b) Number of iterations required to achieve model convergence for EUST-I (closed diamonds) and EUST-II (open diamonds). Simulations for unsteady environmental conditions during sun rise (5–7 h) and sunset (17–22 h) failed to converge as indicated by the hatched areas.

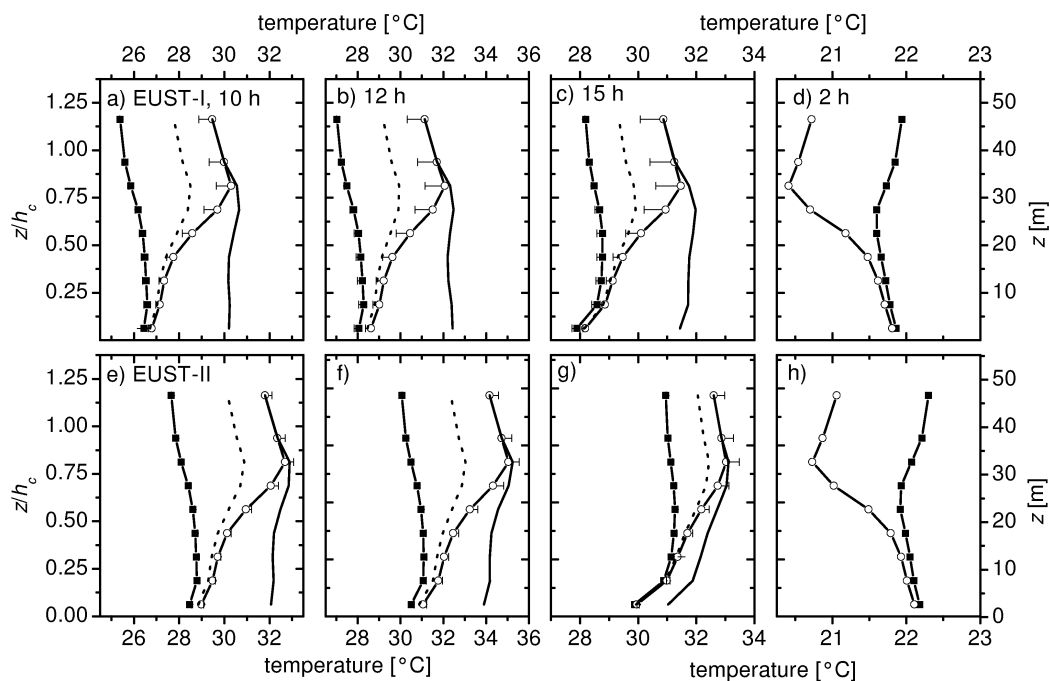


Fig. 3. Predicted vertical profiles of air temperature (line with closed symbols), mean (line with open symbols), sunlit (solid line), and shaded (dotted line) leaf surface temperature for EUST-I (a–d) and EUST-II (e–h) at 10 (a, e), 12 (b, f), 15 (c, g), and 2 h (d, h). Error bars represent predictions using higher stomatal (EUST-I) and lower photosynthesis (EUST-II, see Sect. 2.3 and Table 2) parameters, respectively.

photosynthesis (by decreasing α and θ) leads to decreasing stomatal conductance and results in higher leaf temperatures (0.1–0.5°C) for EUST-II.

The thermal stratification of the canopy air space has also a strong impact on the turbulence regime. The diel pattern of thermal stratification, that has been calculated by the model, is very similar to what we expect for dense vegetations. In the

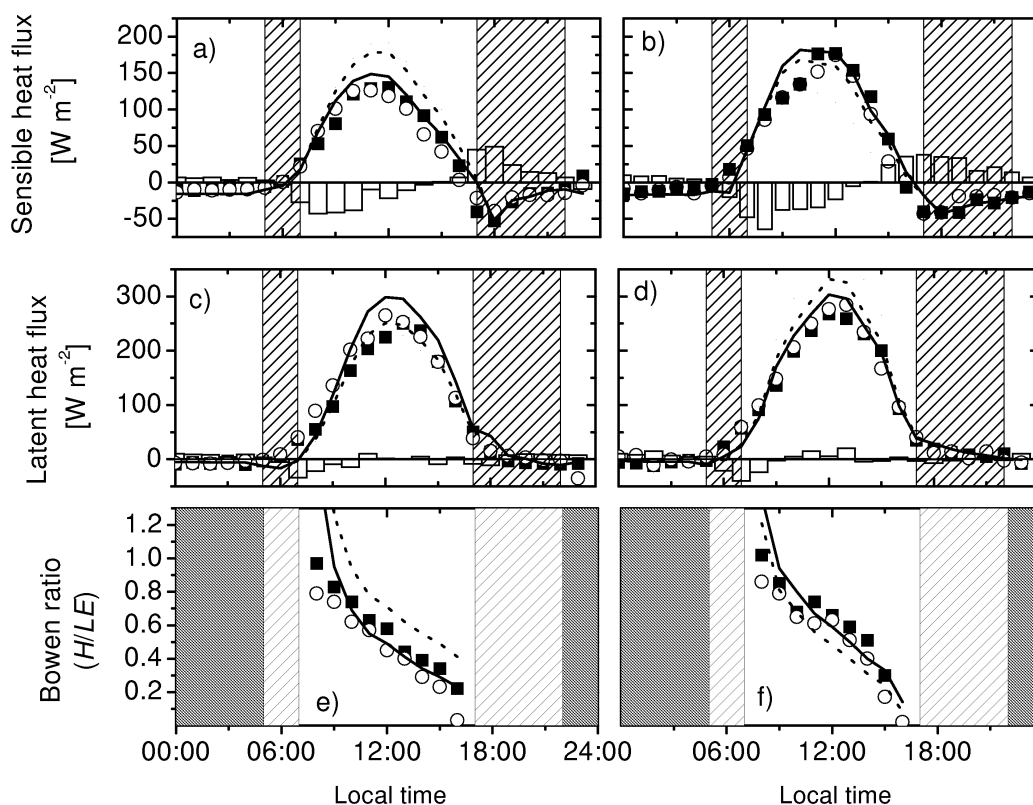


Fig. 4. Comparison of observed and calculated sensible (H) and latent heat flux (LE) and resulting Bowen ratio (H/LE) for EUST-I (a, c, e) and EUST-II (b, d, f). Closed and open symbols represent observations at RBJ-A and RBJ-B towers, respectively. Model calculations are shown for the reference parameterization (dotted line) and modified physiology (solid lines) with increased stomatal conductances (EUST-I) or decreased photosynthesis (EUST-II, see Table 2). (a–d) Column bars represent storage terms for RBJ-A (ΔS calculated as described in Sect. 2.1). For unsteady conditions at sunrise and sunset (hatched area), the numerical scheme is terminated after one iteration (see Fig. 2). (e, f) Only values for daytime conditions are shown.

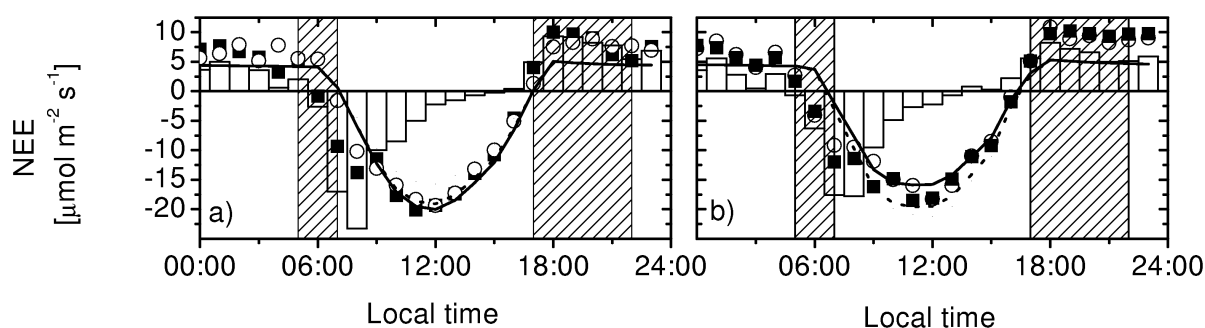


Fig. 5. Comparison of observed and calculated net ecosystem exchange of CO_2 (NEE) for EUST-I (a) and EUST-II (b). Closed and open symbols represent observations at RBJ-A and RBJ-B towers, respectively. Model calculations are shown for the reference parameterization (dotted line) and modified physiology (solid lines) with increased stomatal conductances (EUST-I) or decreased photosynthesis (EUST-II, see Table 2). Column bars represent storage terms for RBJ-A (ΔS calculated as described in Sect. 2.1). For unsteady conditions at sunrise and sunset (hatched area), the numerical scheme is terminated after one iteration (see Fig. 2).

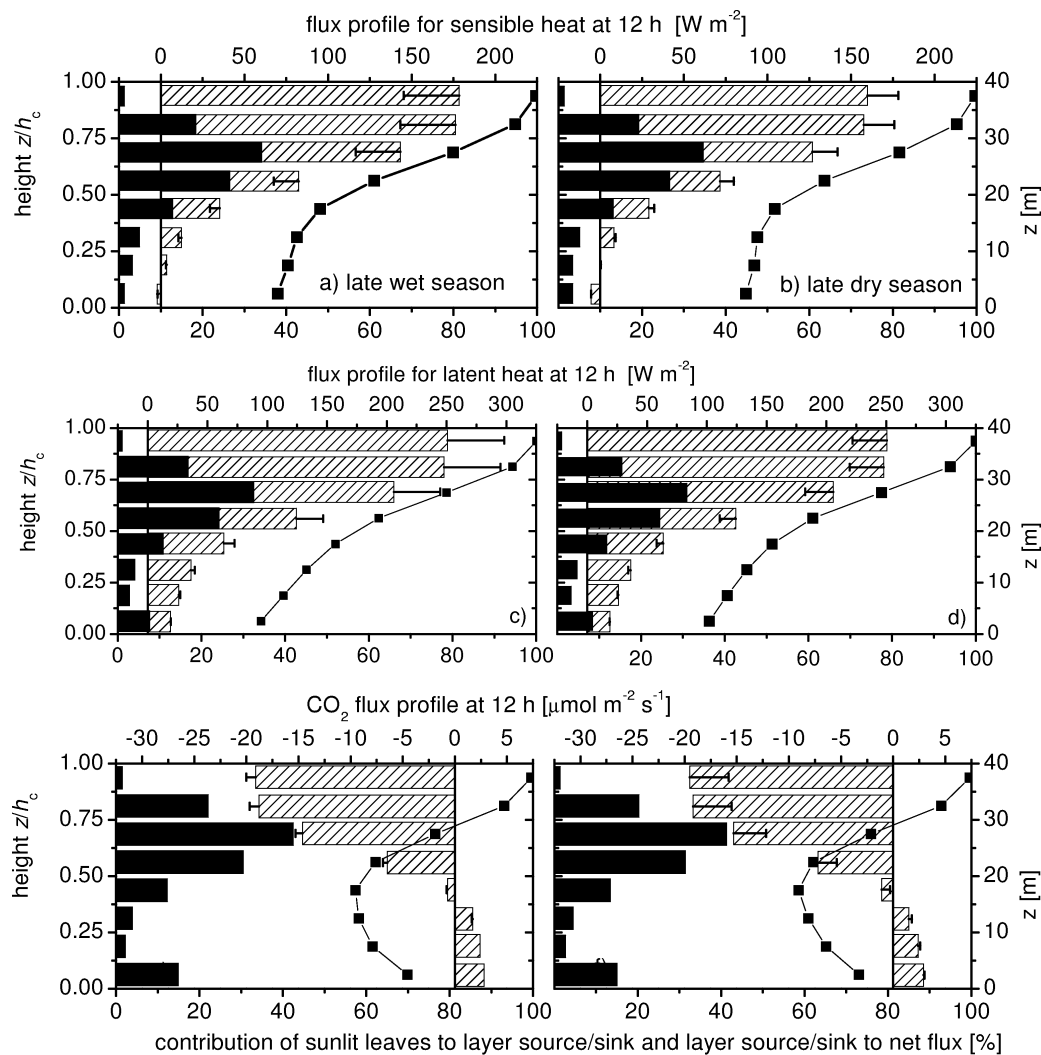


Fig. 6. Midday (12 h) flux profiles (hatched bars) for EUST-I (**a, c, e**) and EUST-II (**b, d, f**), relative source/sink distribution (black bars, sum=100%) and contribution of sunlit leaves to layers source (solid line with closed squares) for sensible heat (**a, b**), latent heat (**c, d**) and CO₂ (**e, f**) for the reference parameterization and a seasonally specific physiology (error bars) with increased stomatal conductances (EUST-I) or decreased photosynthesis (EUST-II).

early morning, the soil surface is warmer than the canopy air above. Later in the day, the foliage is being heated by solar radiation resulting in an unstable stratification of the surface layer above. Since the maximum of absorbed radiation occurs in the upper canopy, the lower canopy layer remains cooler and becomes stable up to 10 m height ($0.25 h_c$). During the night, the stratification in the atmospheric boundary-layer is usually very stable because the surface layer is cooler than the air above (Stull, 1988). However, within dense canopies, the stratification is reversed, because the maximum cooling effect occurs in the upper canopy where biomass is most dense. In combination with soil heat storage, a weak but efficient convective energy flux is generated in the lower canopy (see Jacobs et al., 1994; Kruijt et al., 2000; Simon et al., 2005b).

3.2 Seasonal exchange of CO₂ and energy

The modeled sensible heat (H) and latent heat (LE) fluxes, net ecosystem exchange of CO₂ (NEE) and vertical scalar profiles of H₂O and CO₂ obtained for EUST-I and EUST-II meteorology are compared to observations at the two towers RBJ-A and RBJ-B. The diel cycles of the net fluxes are shown in Figs. 4 and 5. The calculated midday vertical source/sink distributions, flux profiles and the relative contribution of sunlit leaves to the exchange of single canopy layers are shown in Fig. 6. The eddy covariance fluxes measured above the canopy ($F(EC)$) have been corrected for the canopy storage ΔS (see Sect. 2.1).

For both seasonal periods, 50–80% of the available energy at the canopy surfaces is converted into latent heat (LE), especially later during the day. The observed and calculated diel cycles of the Bowen ratio show a strong decline from values close to one just after sunrise to values <0.3 just before sunset. In the early morning and late afternoon, ΔS is large, especially for CO_2 , exceeding even the net flux measured above the canopy. For H and LE , ΔS contributes 40–60 $W\ m^{-2}$. There is generally a good agreement between the RBJ-A and RBJ-B tower EC measurements and storage fluxes. The sensible heat and CO_2 fluxes measured at RBJ-A in the afternoon and morning hours, respectively, are slightly higher compared to RBJ-B, whereas morning LE fluxes are slightly lower ($<4\%$). This variability may result from different tower source areas and reflect the measurement uncertainty (for a discussion of the source area and fetch conditions at RBJ-A see Rummel, 2005).

Generally, a good agreement is obtained between model calculated fluxes and observations, especially when seasonal physiological changes are considered. The meteorological changes from EUST-I to EUST-II (Fig. 1) result in larger energy fluxes and Bowen ratios (i.e. increased fractions of sensible heat) and lower assimilation rates (in relation to the incoming radiation, see Fig. 5). Using the reference parameterization (see Sect. 2.3), the model predicts $\approx 20\%$ larger sensible heat fluxes for EUST-I compared to observations (see also changes in the Bowen ratio shown in Fig. 4i–j). Increasing stomatal conductances for EUST-I, leads to a better agreement between model calculations and observations, but also to a slight overestimation of LE . For midday conditions, this corresponds to a shift in the energy budget: LE increases and H decreases by 50 $W\ m^{-2}$ compared to the model calculations using the reference parameterization (Fig. 6). For the calculated NEE this modification is less important since net assimilation is less sensitive to the modified stomatal parameter than H and LE (see Table 2, see also Simon et al., 2005a).

Reducing the photosynthesis parameters for EUST-II, results in a 10–20% decrease of NEE in absolute numbers and a better agreement between model calculations and observations. The absolute peak NEE at noon time is reduced from 19.5 to 15.8 $\mu\text{mol}\ m^{-2}\ s^{-1}$ (Fig. 6f). The large contribution of net assimilation by sunlit leaves ($>60\%$) in relation to the sunlit leaf surface in the lower canopy ($<5\%$) highlights the non-linearity of photosynthetic light response and the significance of a two-stream canopy radiation model (see Simon et al., 2005a). For sensible and latent heat this effect is less pronounced and the contribution of shaded leaves to the energy fluxes of the lower canopy is larger (40–60%). The maximum source/sink strength for sensible heat, latent heat and net assimilation is located in the upper canopy at 25–30 m with contributions of approximately 35, 33, and 43% to the canopy net flux, respectively. The location of the maxima coincides with the maximum leaf area density several meters below the maximum of foliage temperature (Fig. 3).

The nighttime energy fluxes are generally small, especially for latent heat, and the modifications of physiological parameters have no effect because the modeled nighttime stomatal conductance and leaf CO_2 exchange depend only on minimum stomatal conductance ($g_{s0}=0.01\ \text{mol}\ m^{-2}\ s^{-1}$) and the dark respiration rate. The modeled nighttime sensible heat fluxes are within a range of 10–30 $W\ m^{-2}$ and agree well with observed values. The modeled nighttime CO_2 flux ($\approx 4.5\ \mu\text{mol}\ m^{-2}\ s^{-1}$) is significantly smaller compared to the observations ($NEE\approx 6.5$, $F_{CO_2}(EC)\approx 3.2$, storage term $\Delta S_{CO_2}\approx 3.3\ \mu\text{mol}\ m^{-2}\ s^{-1}$), especially if one considers, that the Eddy Correlation method tends to underestimate nighttime CO_2 fluxes (Goulden et al., 1996; Mahrt, 1999; Araujo et al., 2002; Simon et al., 2005b).

Obviously, the algorithm to calculate respiration by leaves has to be improved (see also Brooks and Farquhar, 1985; Lloyd et al., 1995b). However, according to our knowledge no operational model is available to treat light and dark respiration appropriately at the process level. Furthermore, there are additional CO_2 sources like stem respiration and decomposition of coarse litter (dead trunks and branches $>10\ \text{cm}$ diameter), which are not yet considered in the model. According to Chambers et al. (2000), the coarse litter inputs in central Amazon forests are at least 30% of total surface litter production, which would increase the soil respiration term in our calculations by $\approx 1\ \mu\text{mol}\ m^{-2}\ s^{-1}$. Also for central Amazon forest, Chambers et al. (2004) estimated a mean stem respiration of $1.1\ \mu\text{mol}\ m^{-2}\ s^{-1}$. When these two terms are included in our model calculations the agreement with the observed total respiration is quite well.

For a detailed analysis of the observed and calculated scalar profiles, the period from 14–15 h has been selected, because the afternoon storage fluxes are relatively small (see Figs. 4, 5). A comparison of the observed and modeled CO_2 and H_2O concentration profiles is shown in Fig. 7. In general, the seasonal and diurnal variabilities are not very large and the selected profiles represent typical patterns for day-time conditions. Since the largest emission and uptake rates for H_2O and CO_2 , respectively, usually coincide with the highest turbulence intensities around noon time, increased vertical gradients are counterbalanced by enhanced vertical mixing rates. Since the whole vegetation layer represents a strong H_2O source during the day, H_2O concentrations increase with decreasing height and reach maximum values close to the soil surface where turbulent mixing is weak. As shown in Fig. 7a, b, the modeled H_2O profiles agree with the EUST-I and EUST-II observations and can also explain the steeper H_2O gradients near the soil surface observed during the drier period (EUST-II). A good agreement between observations and model predictions is also obtained for the day-time CO_2 concentration profiles. Consistent with observations, the modeled vertical gradient changes its sign at $\approx 10\ \text{m}$ above ground, where CO_2 uptake by the vegetation balances the emission by the soil. Although soil CO_2 emissions are much lower than the uptake by the vegetation, gradients (with

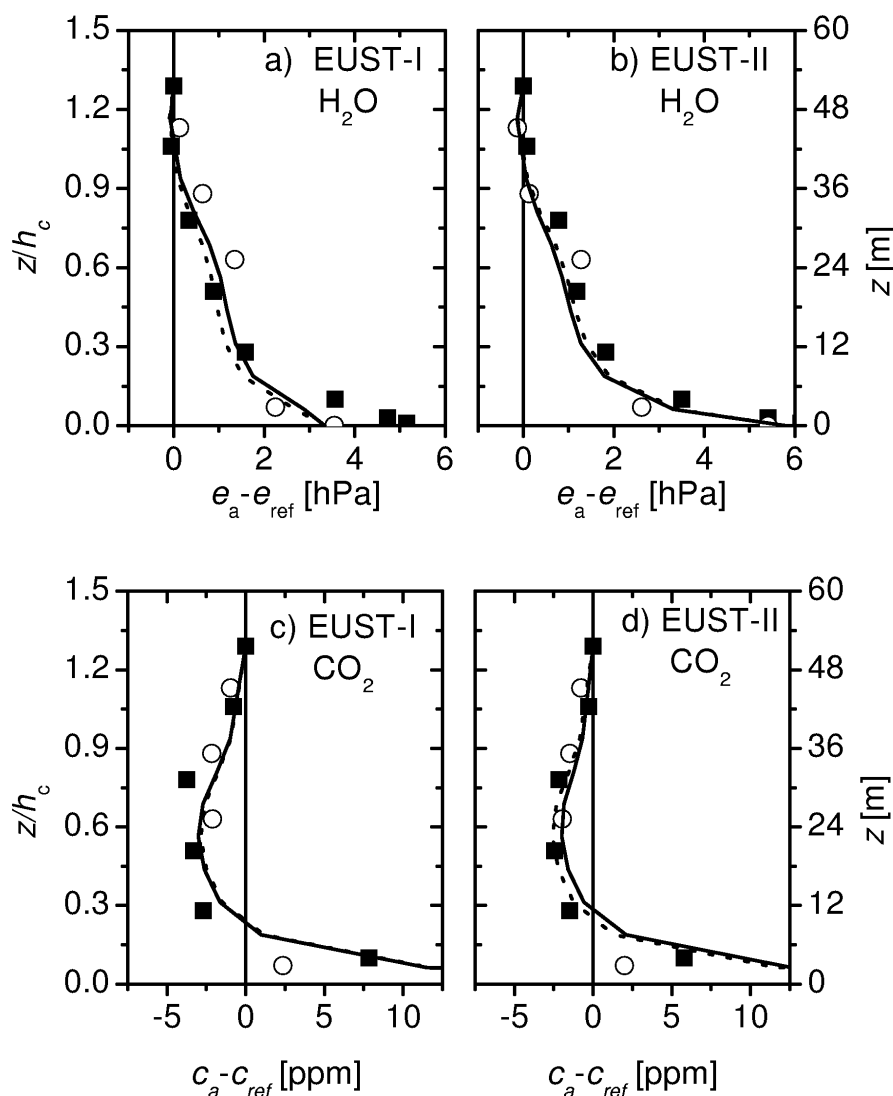


Fig. 7. Comparison of mean observed (RBJ-A: closed squares, RBJ-B open circles) and calculated H₂O (a, b) and CO₂ (c, d) concentration profiles at daytime (14 h) for EUST-I (a, c) and EUST-II (b, d, reference parameterization: dotted line, modified parameterization: solid lines, see Sect. 2.3).

respect to z_{ref}) above 10 m are smaller due to much higher ventilation rates. For both, H₂O and CO₂, the modeled vertical profile is rather insensitive to modifications of the physiological parameters for stomatal conductance and photosynthesis (in contrast to the net fluxes as shown in Simon et al., 2005a).

For nighttime conditions, the environmental conditions are most likely not in steady-state, as indicated by large storage terms, especially for CO₂ (see Figs. 4a, b, e, f and 5a, b). For H₂O, the observed vertical gradients are close to zero and the differences between the measurements made at both towers are larger than the differences between calculations and observations (results not shown). In the case of CO₂, the model

fails to predict the observed CO₂ gradients in size and shape (Fig. 8). The observed concentrations are much higher than model predictions. Possible reasons for the underestimation of the nighttime CO₂ profiles by the model have been investigated by conducting a sensitivity analysis including four parameters:

- As mentioned above, the nighttime CO₂ flux is probably underestimated because the approach to calculate leaf dark respiration may be not fully appropriate. Therefore, leaf respiration was increased to 200% in scenario 1.

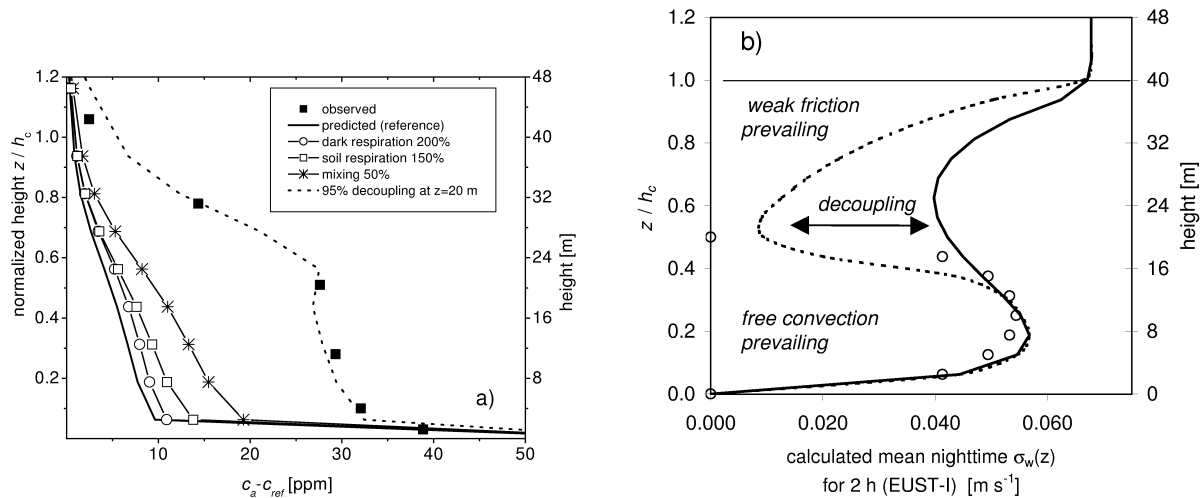


Fig. 8. Comparison of observed and calculated nighttime CO_2 concentration profiles (RBJ-A tower, EUST-I). **(a)** Mean observed profiles (closed squares) compared to model predictions for no parameter modification (solid line), 100% increased dark respiration (line with open circles), 50% increased soil respiration (line with open squares), a 50% reduction of friction induced turbulence (line with stars), and decoupling between the lower and upper canopy (dotted line) assuming an inflection of the $\sigma_w(z)$ profile, as shown b). **(b)** Calculation of $\sigma_w(z)$ for mean nighttime conditions at 2 h during EUST-I (median $\sigma_{w\text{ref}} = 0.068 \text{ m s}^{-1}$) using the original (solid line) and a modified (dotted line) parameterization. Additionally, the parameterization of Garrat (1992), originally derived for the convective boundary-layer is shown (open circles). A decoupling height of 20 m is applied, where $\sigma_w(z)$ is reduced by 22% compared to the original parameterization.

- For the modeled soil respiration, we assume an uncertainty of 50%, which may significantly contribute to near-surface CO_2 concentrations. Therefore soil respiration was increased to 150% in scenario 2.
- A statistical analysis of the input data showed generally a good agreement between the arithmetic mean and median values for all input parameters, except for the standard deviation of vertical wind speed above the canopy ($\sigma_{w\text{ref}}$), which represents the main forcing parameter of turbulent mixing (Raupach, 1989, see also Simon et al., 2005b). As a consequence of a few “untypical” nighttime cases with high turbulence, the arithmetic mean of $\sigma_{w\text{ref}}$ for nighttime conditions is 40% larger compared to its median value. Therefore, we considered a 50% lower value of $\sigma_{w\text{ref}}$ in scenario 3.
- From comprehensive studies on in-canopy turbulence at the Jaru site (Kruijt et al., 2000; Rummel, 2005) it is well known, that the upper and lower canopy layer are strongly decoupled, especially during nighttime. The most frequent turbulent eddies induced by surface-layer friction are too weak and their length scale is too small to reach the lower canopy. This means that vertical transport across a “decoupling height” within the canopy is suppressed. We estimated the potential impact of this effect on vertical scalar dispersion, by modifying the parameterization of the dispersion matrix (see Simon et al., 2005b), assuming 80% inflection of the

profile of the standard deviation of vertical wind speed $\sigma_w(z)$ at $0.5 h_c$ (scenario 4, see also Fig. 8b).

The results of the sensitivity analysis are shown in Fig. 8a. Neither increased leaf, nor increased soil respiration are sufficient to produce large vertical gradients within the canopy compared to the original parameterization. Whereas the effect of leaf respiration is generally small, increased soil respiration affects mainly the CO_2 gradients close to the ground. In contrast, the modeled profile is very sensitive to reduced turbulence which increases the gradients $c_a - c_{\text{ref}}$ by almost 100%. However, this effect is not sufficient to explain the observed shape of the CO_2 profile, which shows small gradients in the lower canopy and a steep decrease of CO_2 concentration above $0.5 h_c$. The inflection of $\sigma_w(z)$ increased the vertical dispersion coefficient (in units of a resistance) across the layer from 17.5 to 22.5 m by $\approx 95\%$ (scenario 4). This strong decoupling effect increased the calculated CO_2 concentration in the lower canopy by a factor of two and may explain, in combination with the effect of weak turbulence (median instead of average value of $\sigma_{w\text{ref}}$), the observed profile very well.

A comparison of the original and modified $\sigma_w(z)$ parameterization is shown in Fig. 8b, calculated using the original and modified parameterization, is shown in Fig. 8b. The maximum in the lower canopy results from the convective part of the calculations and is almost as high as $\sigma_{w\text{ref}}$ above the canopy. The modification of $\sigma_w(z)$ seems realistic. For the lower canopy, it predicts a profile shape which resembles

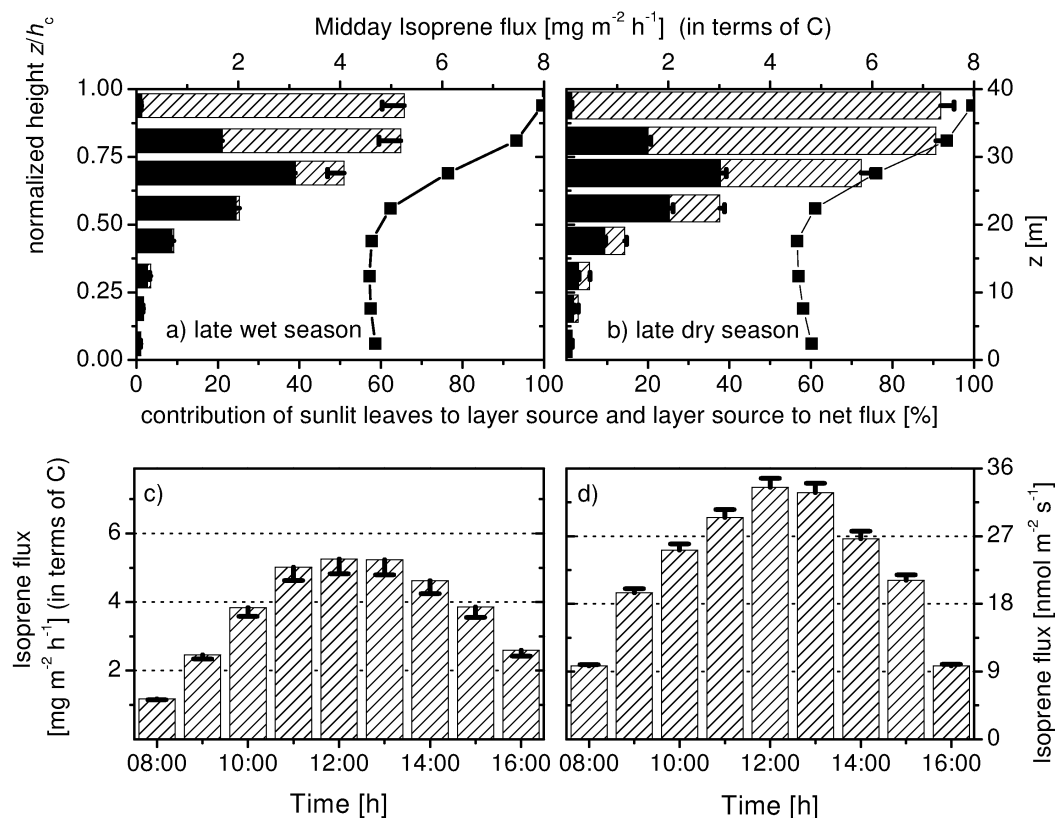


Fig. 9. Predicted isoprene emissions using a standard emission factor of $24 \mu\text{g C g}^{-1} \text{h}^{-1}$ and a specific leaf weight of 125 g m^{-2} . Chemical reactions and deposition are not considered. Midday (12 h) isoprene flux profile (hatched bars) for EUST-I (a) and EUST-II (b), relative source distribution (black bars, sum=100%) and contribution of sunlit leaves to layers source (solid line with closed squares). Diurnal course of isoprene net flux for EUST-I (c) and EUST-II (d). The model is applied using the reference parameterization and modified parameterizations (error bars), implying increased stomatal conductance rates for EUST-I and decreased net assimilation rates for EUST-II (see Table 2).

a parameterization for the convective boundary-layer given by Garrat (1992). Furthermore, the inflection is probably missed by the $\sigma_w(z)$ profile measurements, which have been used for model parameterization, as only 4 profile levels below h_c have been available (see Simon et al., 2005b) and because the relative measurement uncertainty is large in case of $\sigma_w(z) < 0.1 \text{ m s}^{-1}$. Weak turbulent mixing during nighttime has also a strong effect on CO_2 storage inside the canopy volume. For the period from 23–4 h a steady accumulation of CO_2 was observed at all profile levels. Mean $c_{\text{ref}}(t)$ observed above the canopy increases linearly with a constant rate of 8.4 ppm h^{-1} from 416 ppm at 23 h to 458 ppm at 4 h ($r^2=0.98$) predicting a bulk storage flux of $\approx 5 \mu\text{mol m}^{-2} \text{s}^{-1}$ (see also Fig. 1). The temporal evolution dC/dt at all profile heights (see Sect. 2.1), predicts a mean storage flux of $3.3 \mu\text{mol m}^{-2} \text{s}^{-1}$ (see Fig. 5a).

These results show that during nighttime the processes involved in CO_2 exchange (emission and vertical mixing), and most likely other tracer gases, are not in balance which puts the application of a steady-state model for nighttime condi-

tions into question. However, the observed scalar profiles of CO_2 can be explained by decelerated mixing rates and a strong decoupling between the lower and upper canopy. Below 20 m, the vertical gradients are very small (except the gradient at the soil surface, see Fig. 8b), due to efficient vertical mixing by free convective turbulence, which is considered in the turbulence parameterization of our model (see Simon et al., 2005b). Above this “decoupling height”, the CO_2 concentration decreases rapidly by $\approx 30 \text{ ppm}$, due to the stable thermal stratification and weak turbulence mixing. For future model applications, it would be worthwhile, to prove these findings by measurements and, eventually identify the exact location and scale of the nighttime decoupling layer. Other processes involved in nighttime exchange, i.e. horizontal flux divergence (“drainage flow”), have to be considered as well, but are beyond the scope of the present study.

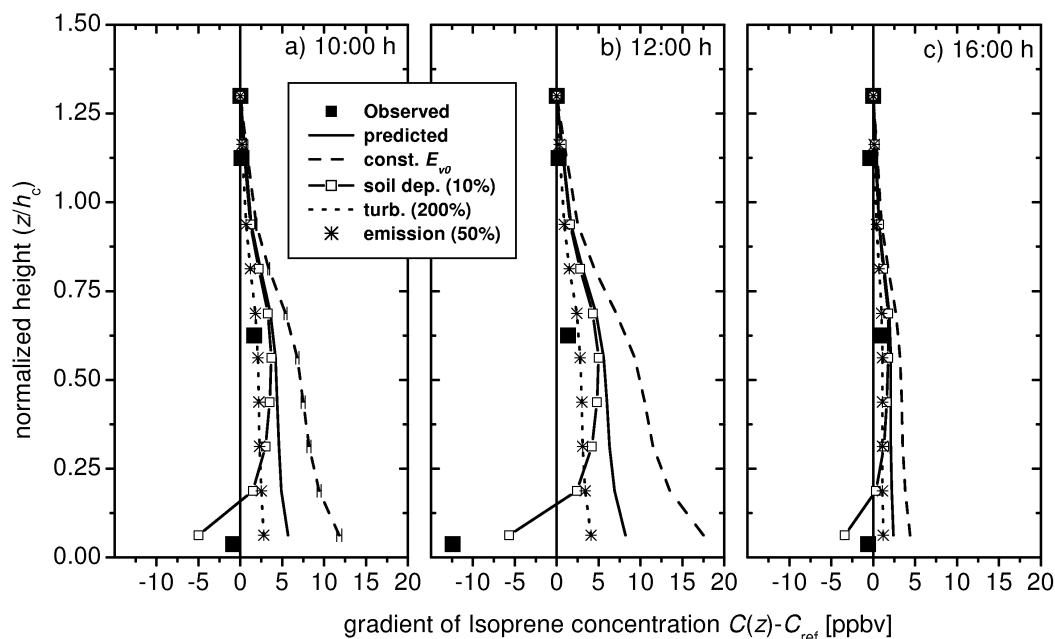


Fig. 10. Comparison of observed (closed squares) and modeled profiles of isoprene concentration on 28/29 October at RBJ-A (EUST-II). Predictions are obtained by applying the algorithm of Guenther et al. (1995) and a light acclimation of the standard emission factor E_{v0} according to Eq. (1) (solid line), a constant E_{v0} in all canopy layers (dashed line), a soil deposition of 10% of the total canopy source (line with square, soil dep.), 100% increased friction induced turbulence (dotted line, turb.), and a 50% reduction E_{v0} (stars).

3.3 Seasonal exchange of isoprene

Isoprene emission was calculated according to the algorithm of Guenther et al. (1993) and the parameterization of the standard emission factor as described in Sect. 2.3. A seasonal comparison of the modeled vertical flux profile and source distribution at noontime (where emissions reach usually maximum values) and the diurnal course of canopy fluxes for EUST-I and EUST-II are shown in Fig. 9. The calculated maximum midday canopy flux of isoprene ranges from 4.8 to 7.5 mg C m⁻² h⁻¹. In general, these numbers agree with recent canopy scale observations of isoprene emission fluxes in Amazonia. Greenberg et al. (2004) derived midday flux values for three sites in the Amazon basin by inverting boundary-layer concentration profiles, which had been measured by tethered balloons. Our calculations lie within their range estimated for the Jaru site in Rondônia (9.8 mg C m⁻² h⁻¹), and two other sites (2.2 and 5.3 mg C m⁻² h⁻¹). For Tapajós, Santarém (East Amazon basin), Rinne et al. (2002) obtained a value of 6.0 mg C m⁻² h⁻¹ by Eddy Covariance and Eddy Accumulation, whereas Stefani et al. (2000) obtained a value of 4.6 mg C m⁻² h⁻¹ by using the same technique for a site near Manaus (see Harley et al., 2004, for a comparison of observations and emissions from different Neotropical sites).

Compared to energy and CO₂ exchange (Figs. 4–5), changing environmental conditions lead to larger seasonal

variabilities of modeled fluxes. Using the same model parameterization for both periods predicts a 39% increase of midday fluxes for dry season conditions compared to the wet season. Assuming slight physiological changes in the H₂O and CO₂ leaf gas exchange (error bars in Fig. 9) increases the variability to more than 50%. Obviously, a reduction of assimilation for EUST-II, as assumed in our simulations by decreasing the photosynthesis parameters α and θ (Table 2, Fig. 5d), results in increased isoprene fluxes due to higher foliage temperatures, which again are a result of reduced stomatal conductance rates. The shape of the vertical isoprene source distributions (Fig. 9a–b) shows minor seasonal variations. In general, $\approx 85\%$ of the midday net flux is emitted by the upper canopy ($z > 20$ m), whereby $\approx 60\%$ is emitted in the layer between 20 and 30 m where leaf area density is highest. Similarly to net assimilation, the non-linearity of the emission algorithm leads to a large contribution ($> 60\%$) of sunlit leaves to the source strength in all layers, even close to the ground where the fraction of sunlit leaves is small ($< 4\%$).

Concentration measurements made simultaneously at different canopy levels within the canopy during EUST-II have been used to evaluate the predicted isoprene exchange. To assess the sensitivity of the calculated isoprene profiles we compared the observations with model results obtained for the parameterization described in Sect. 2.3 and four additional simulations with the following modifications applied:

1. *No light acclimation of emission capacity:* Despite experimental evidence (see Sect. 2.3), the emission capacity for isoprene and monoterpenes is sometimes treated as a constant bulk value. Therefore we applied a parameterization where the emission capacity is assumed to be constant within the canopy (the factor 2.7 in Eq. (1) is set to zero).
2. *Deposition to soil:* In laboratory studies, it has been shown that significant fractions of isoprene were consumed by soil microbes (Cleveland and Yavitt, 1997, 1998). As a rough estimate, a soil sink equivalent to 10% of the canopy source was applied.
3. *Vertical mixing:* To test the sensitivity of the calculated profile to the vertical mixing rate, a further simulation was applied with increased turbulence (200%, see also Sect. 3.2).
4. *Source uncertainty:* The profile sensitivity to the calculated isoprene source strength was tested by reducing the standard emission factor by 50% (being in the same order of magnitude as its uncertainty, see Harley et al., 2004).

Fig. 10 shows a comparison of observed and modeled profiles for morning (10 h), midday (12 h) and late afternoon (16 h) hours on 28 and 29 October 1999 at RBJ-A. Compared to observations, the model predicts relatively high isoprene concentrations close to the ground. Whereas the observations show the maximum concentrations in the upper canopy close to the sources, the model predicts isoprene accumulation close to the ground, where mixing rates are low. The calculated profiles for the reference case show a much better agreement with observations compared to the simulations, where the emission capacity is assumed to be constant with canopy depth (solid line and dashed lines in Fig. 10, respectively). However, decreasing concentrations in the lower canopy can be obtained only by assuming additional sink processes at the ground (solid line with square symbols in Fig. 10). We have to admit that the applied sink strength for isoprene (10% of canopy emission) is very speculative. The resulting deposition value is one order of magnitude higher compared to the uptake, which would result from the empirical model ($2 \times 10^{-5} \text{ min}^{-1} \text{ g}^{-1}$ for 3 cm active soil depth, 850 kg m^{-3} soil bulk density) given by Cleveland and Yavitt (1998). However, this empirical model is based on few laboratory measurements, which show a large variability, spanning three orders of magnitude.

In contrast to soil deposition, enforced mixing and decreased emissions do not improve the agreement between the calculated and observed shape of the isoprene profiles (dotted line and star symbols in Fig. 10, respectively). Chemical reactions are regarded as unimportant within the timescales under investigation because the expected lifetime of isoprene ($>1 \text{ h}$, see Zimmerman et al., 1988; Guenther et al.,

1995) is larger than characteristic canopy ventilation rates ($<1 \text{ h}$, see Simon et al., 2005b; Rummel, 2005). Furthermore, the chemical loss of isoprene through reaction with OH and ozone occurs mainly in the atmospheric boundary-layer above the canopy (Zimmerman et al., 1988; Greenberg et al., 2004). Simulations with a single-column model which includes the chemical processes (Ganzeveld et al., 2002) have predicted similarly high isoprene concentrations near the soil surface (L. Ganzeveld, personal communication, 2004).

The decrease of emission potential in lower canopy layers results in a 30% reduction of the canopy net fluxes. There is also indirect evidence for this light acclimation of isoprene emission capacity. Several ecological studies in Amazonia have found a large variability of specific leaf weight (SLW), which correlates with the light environment (Reich et al., 1991; Roberts et al., 1993; McWilliam et al., 1993), i.e. the vertical position within the canopy. Since the standard emission factor is normalized on a mass basis, the modeled emission scales with SLW. Carswell et al. (2000) e.g. found at a site near Manaus SLW values of 114 g m^{-2} at the canopy top compared to 69 g m^{-2} close to the ground. This variability alone already explains a 40% decrease of the emissions potential without changing the standard emission factor on a mass basis (see also Guenther et al., 1999).

A simple global isoprene emission estimate for tropical rain forest is obtained by a temporal integration of the mean diel cycles of isoprene fluxes calculated for EUST-I and EUST-II and by spatial integration assuming a globally forested area of 4.33 million km^2 (Guenther et al., 1995). For the two diurnal cycles shown in Fig. 9, this scaling exercise predicts a range of $52.2\text{--}77.1 \text{ Tg C y}^{-1}$, which is somewhat lower than the estimate of 84 Tg C y^{-1} given by Guenther et al. (1995).

3.4 Seasonal exchange of ozone

In contrast to isoprene, the canopy layer represents an important sink rather than a source for ozone. As discussed in detail at the end of Sect. 2.3, chemical reactions with nitrogen oxide have been neglected and ozone destruction by highly reactive BVOC's is not considered in our model calculations (also since we have no informations on the emissions of these highly reactive BVOC's). A comparison of observed and modeled net fluxes and the vertical profiles of cumulative ozone deposition velocity, sink distribution and the contribution of sunlit leaves to the layer sink at noon time is shown in Fig. 11. Net fluxes measured above the canopy have been corrected for canopy storage (Sect. 2.1). Typical observed and calculated concentration profiles for daytime conditions are shown in Fig. 12. The 14 h concentration profile is selected because daytime canopy storage is close to zero in the early afternoon (see Fig. 11c,d).

The maximum uptake occurs at noon time, when ambient concentrations and stomatal conductances reach their

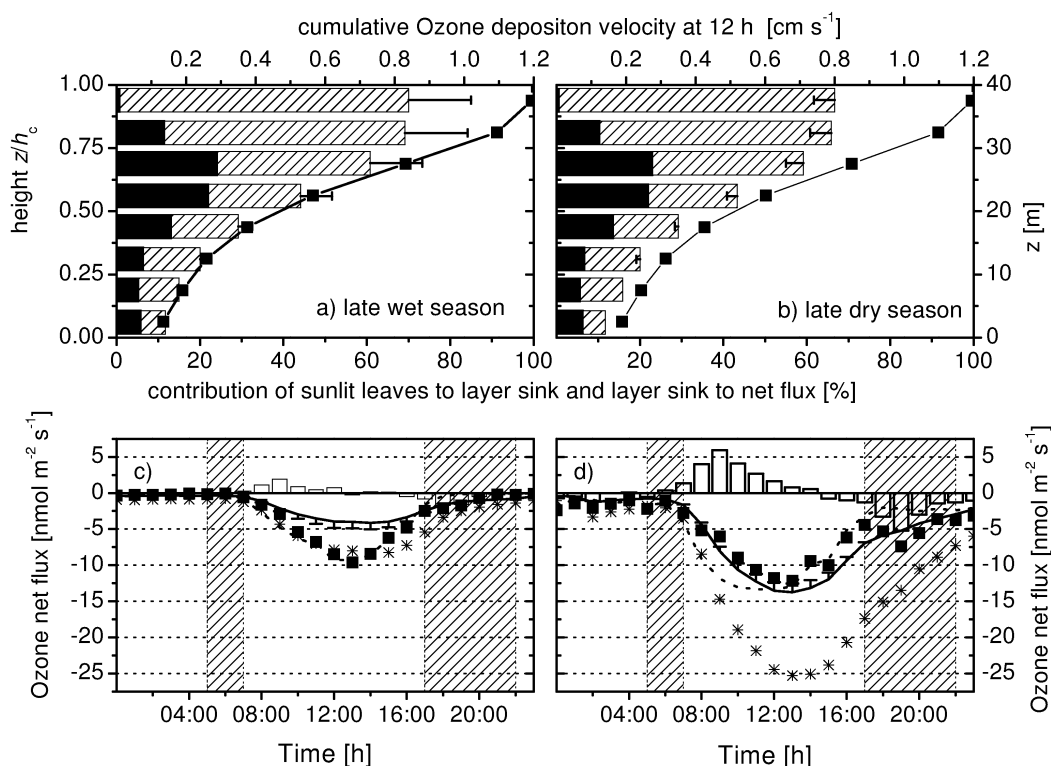


Fig. 11. Predicted ozone deposition for a cuticular resistance of $r_{\text{cut},\text{O}_3}=5000 \text{ s m}^{-1}$ (derived by Rummel, 2005, for EUST-II, see Sect. 2). (a–b) Cumulative ozone deposition velocity (v_{d,O_3} , hatched bars), relative vertical sink distribution (black bars, sum=100%) and contribution of sunlit leaves to layer sink (line with closed squares) for EUST-I (a) and EUST-II (b). (c–d) Comparison of observed (closed squares) and modeled (solid lines) net ozone flux for EUST-I (c) and EUST-II (d). The shaded areas represent unsteady periods during sunrise and sunset (Sect. 3.1). Observations (eddy covariance measurements at RBJ-A tower, dotted lines) are corrected for canopy storage (open bars). The model is applied using the reference parameterization and modified stomatal (EUST-I) and assimilation (EUST-II) parameters (error bars, see Sect. 2.3 and Table 2). A second simulation was performed using a lower cuticular resistance $r_{\text{cut},\text{O}_3}=1000 \text{ s m}^{-1}$ (star symbols).

maxima and the turbulent timescales for ozone transport are low. For EUST-II, significant nighttime fluxes are observed and modeled. In general, the linear correlation between observed and calculated net fluxes is high ($r^2 > 0.92$). However, the results are not consistent for wet and dry season conditions. The linear regression statistics for wet season conditions indicate a systematic underestimation of the observed fluxes ($y=0.44x-0.5$ for the reference parameterization), whereas the agreement between observed and calculated fluxes for dry season conditions is quite good ($y=1.3x+1.2$ for the reference parameterization).

Interestingly, the observed bulk value of the dry deposition velocity v_{d,O_3} (as the observed net flux divided by the concentration above the canopy, see Eq. (2), Table 1, Fig. 11c–d) decreases by more than 60% from EUST-I to EUST-II. For example, the daily mean maximum deposition value, which is typically observed at noon, decreases from 1.98 cm s^{-1} during EUST-I to 0.73 cm s^{-1} during EUST-II. In theory, this must result from a seasonal variability of the leaf resistance to ozone uptake ($r_{\text{leaf},\text{O}_3}$, see Eq. 4), since soil, aerodynamic

and boundary-layer resistances are very similar for both periods (for a comparison of soil resistances see Gut et al., 2002a). However, realistic physiological changes in stomatal conductances and assimilation rates are obviously insufficient to explain the observed variability of v_{d,O_3} , although the disagreement between observations and model calculations are significantly reduced. For a seasonally specific parameterization (see Table 2 in Sect. 2.3) with higher stomatal conductance rates for wet season conditions (EUST-I), the calculated midday deposition velocity increases from 0.8 to 1.05 cm s^{-1} , while for dry season conditions (EUST-II) with reduced assimilation parameters v_{d,O_3} decreases from 0.85 to 0.7 cm s^{-1} .

A closer look on the vertical source/sink distribution shown in Fig. 11a–b gives a potential hint for the disagreement between observed and modeled ozone deposition. The shape of the source/sink distribution of ozone is more uniform compared to isoprene and assimilation because the ozone uptake has a second, cuticular pathway, which is independent of physiological control (Eq. 6). The cuticular

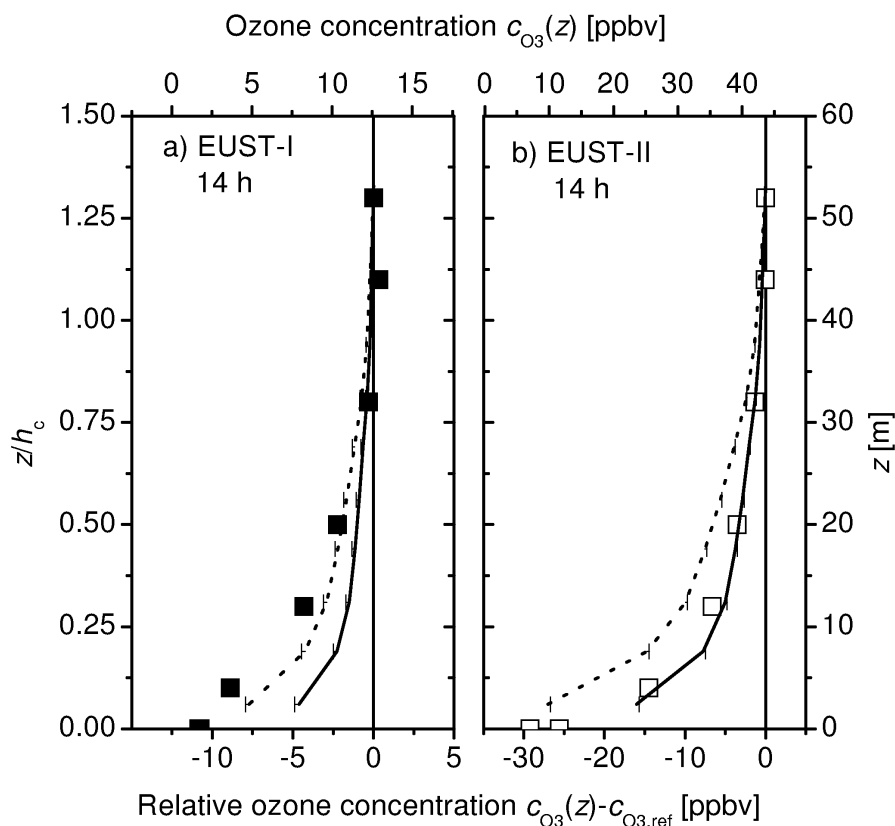


Fig. 12. Comparison of observed (squares) and modeled vertical concentration profiles of ozone during daytime (14 h) for EUST-I (a) and EUST-II (b). Predicted profiles are obtained for the reference parameterization (Sect. 2.3) using a cuticular resistance of $r_{cut,O_3} = 5000 \text{ s m}^{-1}$ (solid lines) and $r_{cut,O_3} = 1000 \text{ s m}^{-1}$ (dotted lines). Error bars (only positive) represent prediction variability for increased stomatal and decreased photosynthesis parameters (see Fig. 11).

uptake is mainly controlled by the available leaf surface area and the resistance to cuticular uptake r_{cut,O_3} . Therefore, the contribution of the lower canopy (0–20 m) and shaded foliage is relatively large compared to assimilation and isoprene emission. In contrast to leaf surface area, where parameter uncertainty is on the order of 10% (see Simon et al., 2005a), the cuticular conductance ($1/r_{cut,O_3}$) is much more uncertain. The value of 5000 s m^{-1} inferred for our site by Rummel (2005) (see Sect. 2.3) is even smaller than minimum g_s , g_{s0} . Accordingly, the parameter uncertainty for non-stomatal ozone deposition is very large. In a recent field study on shoots of Scots pine, Altimir et al. (2004) investigated the important role of non-stomatal uptake processes. Consistently with our results, they observed, for high relative humidity conditions, non-stomatal ozone deposition rates on the order of 50% of the total flux. Even higher non-stomatal ozone deposition rates of 70% and a strong dependence on global radiation and air temperature have been reported by Fowler et al. (2001) for moorland vegetation.

Within this context, we reduced the cuticular resistance to ozone deposition from 5000 to 1000 s m^{-1} . On a first glance this is a drastic change. However, it is still within the uncertainty range of this parameter and can explain the observed wet season deposition rates quite well (Fig. 11a). Consistent with the net fluxes, the modeled ozone concentration profiles for EUST-II show a good agreement with observations using the value of $r_{cut,O_3} = 5000 \text{ s m}^{-1}$, whereas EUST-I observations are strongly underestimated (Fig. 12a). Reducing the cuticular resistance from 5000 to 1000 s m^{-1} increases the calculated fluxes for both seasonal periods by 100%. For EUST-I, this results in a good agreement between observed and calculated concentrations profiles and fluxes, whereas EUST-II observations are overestimated using the lower value of r_{cut,O_3} .

Whereas the stomatal pathway (first part of the right side of Eq. 6) has a strong maximum in the upper canopy and occurs only at the bottom leaf side (hypo-stomatous leaves), the cuticular uptake is linearly related to the leaf area in each layer and occurs at both leaf sides (indicated by the factor of two in the second part on the right side in Eq. 6).

Furthermore, the stomatal pathway is coupled to physiological activity, which is much stronger in the upper canopy (Fig. 11a, b). Consequently, uncertainties of the stomatal pathway can not explain the disagreement between the observed and calculated ozone concentrations in the lower canopy during EUST-I. On the other hand, a strong seasonal variability of $r_{\text{cut},\text{O}_3}$ is unlikely because this implies fundamental changes of leaf structure. In part, the structure and function of leaves changes as a result of lifespan regulation (Reich et al., 1991), which might be synchronized and follow the seasonal cycles of wet and dry periods within evergreen tropical rain forest (see also Malhi et al., 1998). A combination of all the potential factors (leaf physiology, canopy and leaf structure) reduce the observed disagreement between the expected and observed seasonal variability of ozone deposition, but are still insufficient.

Speculating, we may discuss ozone deposition to wetted surfaces during EUST-I, when the climatic conditions have been different. Because the relative humidity during EUST-I were significantly higher compared to EUST-II (see Fig. 1), the ambient air in the lower canopy was nearly saturated with water vapor and large fractions of the leaf surfaces were wetted. The composition and chemistry of the water film on wetted leaf surfaces are not very well understood and deposition models are treating this effect on ozone uptake differently. The earliest models have considered the low solubility of ozone in pure water reducing the ozone uptake of leaves (Chameides, 1987; Baldocchi et al., 1987). However, depending on the origin and composition of the surface water, the opposite effect was also found. Larger than theoretical uptake rates have been observed e.g. on leaf surfaces wetted by dew (Wesely et al., 1990) or rain water (Fuentes et al., 1992), above a deciduous forest in the winter (Padro et al., 1992), and also over oceans (Wesely and Hicks, 2000). In line with those studies, our results indicate that there might be a significant ozone uptake by wet leaf surfaces, under the likely assumption, that larger fractions of the leaf surface were wet during the wet season,

Alternatively to deposition to wet surfaces, chemical loss of ozone due to reaction with highly reactive BVOC's can not be totally excluded (see Sect. 2.3). Assuming a rate constant of $10^{-14} \text{ cm}^3 \text{ molecules}^{-1} \text{ s}^{-1}$ for this type of reaction (see Goldstein et al. 2003), a mean reactive BVOC concentration of $\approx 1.4 \text{ ppb}$ is required to explain the observed ozone fluxes for wet season conditions (i.e. increase from ≈ 5 to $10 \text{ nmol m}^{-2} \text{ s}^{-1}$ for an ozone concentration of $c_{\text{O}_3} \approx 10 \text{ ppb}$). However, if BVOC emissions and concentrations remain constant, this mechanism predicts a much stronger chemical ozone loss of $\approx 20 \text{ nmol m}^{-2} \text{ s}^{-1}$ for dry season conditions (140% increase of the predicted ozone flux) due to four fold higher ozone concentrations ($c_{\text{O}_3} \approx 40 \text{ ppb}$, see Table 1). Therefore, the hypothesis implies additionally a strong seasonal variability of BVOC emissions with at least 50 to 100% increased BVOC emissions for wet compared to dry season conditions, which seems pretty much.

4 Conclusions

The evaluation of biosphere-atmosphere exchange of energy, CO_2 , isoprene and ozone has shown, that the presented approach and parameterization can serve for multiple purposes in ecosystem research on the Amazon rain forest. The observed and modeled net fluxes and concentration profiles are quite consistent. In alignment with observations, the model predicts a stable thermal stratification of the lower canopy during the day, which is reversed during nighttime. For nighttime conditions, the decoupling between the lower and upper canopy is obviously underestimated, leading to a disagreement between observed and predicted CO_2 concentration profiles. However, this may be attributed to the uncertainty of the turbulence parameterization, since the simulated concentration profiles are very sensitive to the standard deviation of vertical wind speed between 0.4 and $0.6 h_c$. The explicit calculation of the temperature and scalar concentrations at the leaf surface, as well as within the canopy air volume is quite significant for the calculated fluxes, as demonstrated for isoprene. The observed seasonal variability of net primary production and transpiration can be explained by a combination of environmental and physiological factors. Direct indications for such changes have been already described in the companion paper (Simon et al., 2005a), where leaf level gas exchange measurements from different seasons are compared. The comparison of observed and modeled in-canopy concentrations of isoprene for dry season and of ozone net fluxes and in-canopy concentrations for wet season conditions highlights two gaps in our current knowledge of canopy processes, which should be investigated in more detail in future studies. First, vertical scaling of isoprene emission capacity is necessary to obtain realistic predictions of isoprene concentrations in the lower canopy. This reduces the emissions fluxes by 30% and should be considered in regional and global modeling studies on isoprene emissions by plants. Secondly, the seasonal comparison of observed and predicted ozone fluxes pointed out the important role of non-stomatal deposition. Increased deposition rates observed for wet season conditions give evidence of important sink processes, which lack of knowledge and are not yet considered in current models. We identified deposition to wetted surfaces and chemical destruction by highly reactive BVOC's as processes which have to be investigated in more detail in future studies. In general, it would be worthwhile to establish ecological principles for the natural variability of leaves, e.g. their optical properties (albedo), the permeability of the leaf cuticula and the regulation of specific dry weight (SLW). The latter does not only affect the calculated emission of isoprene. If shaded leaves have a lower specific weight, they have simultaneously a larger surface and probably a higher permeability for ozone and other trace gases, which would result in a much higher cuticular uptake.

Acknowledgements. We would like to thank U. Kuhn and S. Rottenberger for providing the isoprene concentration profile measurements and B. Kruijt and J. Elbers from Alterra-Institute for providing the flux and concentration profile data from the towers in Rondônia. We thank the two reviewers for comments on a previous version of this manuscript. The research is supported by the Max Planck Society and the European Union (EUSTACH-LBA; ENV4-CT97-0566).

Edited by: A. Goldstein

References

- Altimir, A., Tuovinen, J.-P., Vesala, T., Kulmala, M., Hari, P.: Measurements of ozone removal by scots pine shoots: calibration of a stomatal uptake model including the non-stomatal component, *Atmos. Environ.* 38, 2387–2398, 2004.
- Andreae, M. O., Artaxo, P., Brandao, C., Carswell, F. E., Ciccioli, P., da Costa, A. L., Culf, A. D., Esteves, J. L., Gash, J. H. C., Grace, J., Kabat, P., Lelieveld, J., Malhi, Y., Manzi, A. O., Meixner, F. X., Nobre, A. D., Nobre, C., Ruivo, M., Silva-Dias, M. A., Stefani, P., Valentini, R., von Jouanne, J., and Waterloo, M. J.: Biogeochemical cycling of carbon, water, energy, trace gases, and aerosols in Amazonia: The LBA-EUSTACH experiments, *J. Geophys. Res.*, 107, 33.1–33.25, 2002.
- Araujo, A., Nobre, A., Kruijt, B., Elbers, J., Dallarosa, R., Stefani, P., von Randow, C., Manzi, A., Culf, A., Gash, J., Valentini, R., and Kabat, P.: Comparative measurements of carbon dioxide fluxes from two nearby towers in a central Amazonian rainforest: The Manaus LBA site, *J. Geophys. Res.*, 107, 58.1–58.20, 2002.
- Bakwin, P., Wofsy, S., Fan, S.-M., Keller, M., Trumbore, S., and Da Costa, J.: Emission of nitric oxide (NO) from tropical forest soils and exchange of NO between the forest canopy and atmospheric boundary layers, *J. Geophys. Res.*, 95, 16 755–16 764, 1990.
- Baldocchi, D.: A Lagrangian random-walk model for simulating water vapour, CO₂ and sensible heat flux densities and scalar profiles over and within a soybean canopy, *Bound.-Layer Meteorol.*, 61, 113–144, 1992.
- Baldocchi, D. and Meyers, T.: On using eco-physiological, micrometeorological and biogeochemical theory to evaluate carbon dioxide, water vapor and trace gas fluxes over vegetation – a perspective, *Agric. For. Meteorol.*, 90, 1–25, 1998.
- Baldocchi, D., Hicks, B., and Camara, P.: A canopy stomatal-resistance model for gaseous deposition to vegetated surfaces, *Atmos. Environ.*, 21, 91–101, 1987.
- Baldocchi, D., Fuentes, J. D., Bowling, D. R., Turnipseed, A. A., and Monson, R. K.: Scaling isoprene fluxes from leaves to canopies: Test cases over a boreal aspen and a mixed species temperate forest, *J. Appl. Meteorol.*, 38, 885–898, 1999.
- Bosveld, F., Holtslag, A., and Van den Hurk, B.: Nighttime convection in the interior of a dense douglas forest, *Bound.-Layer Meteorol.*, 93, 171–195, 1999.
- Brooks, A. and Farquhar, G.: Effect of temperature on the CO₂/O₂ specificity of Ribulose-1,5-bisphosphate carboxylase/oxygenase and the rate of respiration in the light. Estimates from gas-exchange measurements on spinach., *Planta*, 165, 397–406, 1985.
- Carswell, F., Meir, P., Wandell, E., Bonates, L., Kruijt, B., Barbosa, E., Nobre, A., Grace, J., and Jarvis, P.: Photosynthetic capacity in a central Amazonian rain forest, *Tree Physiol.*, 20, 179–186, 2000.
- Carswell, F., Costa, A., Palhete, M., Mahli, Y., Meir, P., Costa, d. P., Ruivo, M. d. L., Leal, L. d. D., Costa, J., Clement, R., Grace, J.: Seasonality in CO₂ and H₂O flux at eastern Amazonian rain forest, *J. Geophys. Res.*, 107(D20), 43.1–43.16, 2002.
- Chambers, J. Q., Higuchi, N., Schimel, D. S., Ferreira, L. V., Melack, J.: Decomposition and carbon cycling of dead trees in tropical forests of the central Amazon, *Oecologia* 122, 380–388, 2000.
- Chambers, J. Q., Tribuzy, E. S., Toledo, L. C., Crispim, B. F., Higuchi, N., Dos Santos, H., Araujo, A., Kruijt, B., Nobre, A. D., Trumbore, S. E.: Respiration from a tropical forest ecosystem: partitioning of sources and low carbon use efficiency, *Ecological Applications* 14 (4, Supplement), 72–88, 2004.
- Chameides, W.: Acid dew and the role of chemistry in the dry deposition of reactive gases to wetted surfaces, *J. Geophys. Res.*, 92, 11 895–11 908, 1987.
- Chameides, W.: The chemistry of ozone deposition to plant leaves: role of ascorbic acid, *Env. Sci. Technol.*, 23, 595–600, 1989.
- Chameides, W. L. and Lodge, J. P.: Tropospheric ozone: formation and fate, in: *Surface Level Ozone Exposures and their Effects on Vegetation*, edited by: Lefohn, A., pp. 1–30, Lewis publishers, USA, 1992.
- Cleveland, C. C. and Yavitt, J. B.: Consumption of atmospheric isoprene in soil, *Geophys. Res. Lett.*, 24, 2379–2382, 1997.
- Cleveland, C. C. and Yavitt, J. B.: Microbial consumption of atmospheric isoprene in a temperate forest soil, *Appl. Env. Microbiol.*, 64, 172–177, 1998.
- Fowler, D., Flechard, C., Cape, J. N., Storeton-West, R. L., Coyle, M.: Measurements of ozone deposition to vegetation quantifying the flux, the stomatal and non-stomatal components, *Water Air Soil Pollut.* 130, 63–74, 2001.
- Fuentes, J., Gillespie, T., Hartog, G. D., and Neumann, H.: Ozone deposition onto a deciduous forest during dry and wet conditions, *Agric. For. Meteorol.*, 62, 1–18, 1992.
- Ganzeveld, L. and Lelieveld, J.: Dry deposition parameterization in a chemistry general circulation model and its Influence on the distribution of reactive trace gases, *J. Geophys. Res.*, 100, 20 999–21 012, 1995.
- Ganzeveld, L., Lelieveld, J., Dentener, F., Krol, M., and Roelofs, G.-J.: Atmosphere-biosphere trace gas exchange simulated with a single-column model, *J. Geophys. Res.*, 107, 8.1–8.21, 2002.
- Garrat, J.: *The Atmospheric Boundary Layer*, Cambridge Atmospheric and Space Science Series, Cambridge University Press, Cambridge, 1992.
- Geron, C., Guenther, A., and Greenberg, J.: Biogenic volatile organic compound emissions from a lowland tropical wet forest in Costa Rica, *Atmos. Environ.*, 36, 3793–3802, 2002.
- Goldstein, A., McKay, M., Kurpius, M., Schade, G. W., Lee, A., Holzinger, R., Rasmussen, R.: Forest thinning experiment confirms ozone deposition to forest canopy is dominated by reaction with biogenic VOCs, *Geophys. Res. Lett.*, 31(L22106), 1–4, 2004.
- Goulden, M., Munger, J., Fan, S.-M., Daube, B., and Wofsy, S.: Measurements of carbon sequestration by long-term eddy covariance: Methods and a critical evaluation of accuracy, *Global*

- Change Biol., 2, 169–182, 1996.
- Grace, J., Lloyd, J., McIntyre, J., Miranda, A., Meir, P., Miranda, H., Moncrieff, J., Massheder, J., Wright, I., and Gash, J.: Fluxes of carbon dioxide and water vapour over an undisturbed tropical rain forest in south-west Amazonia, *Glob. Clim. Change*, 1, 1–12, 1995.
- Greenberg, J., Guenther, A., Petron, G., Wiedinmyer, C., Vega, O., Gatti, L., Tota, J., and Fisch, G.: Biogenic VOC emissions from forested Amazonian landscapes, *Global Change Biol.*, 10, 1–12, 2004.
- Guenther, A., Zimmerman, P., Harley, P., Monson, R., and Fall, F.: Isoprene and monoterpene emission rate variability: Model evaluations and sensitivity analysis, *J. Geophys. Res.*, 98, 12 609–12 617, 1993.
- Guenther, A., Hewitt, C., Erickson, D., Fall, R., Geron, C., Graedel, T., Harley, P., Klinger, L., Lerdau, M., McKay, W., Pierce, T., Scholes, B., Steinbrecher, R., Tallamraju, R., Taylor, J., and Zimmerman, P.: A global model of natural volatile organic compound emissions, *J. Geophys. Res.*, 100, 8873–8892, 1995.
- Guenther, A., Baugh, B., Brasseur, G., Greenberg, J., Harley, P., Klinger, L., Serca, D., Vierling, L.: Isoprene emission estimates and uncertainties for the central african expresso study domain, *J. Geophys. Res.*, 104(D23), 30 625–30 639, 1999.
- Gut, A., Scheibe, M., Rottenberger, S., Rummel, U., Welling, M., Ammann, C., Kirkman, G., Kuhn, U., Meixner, F., Kesselmeier, J., Lehmann, B., Schmidt, J., Müller, E., and Piedade, M.: Exchange of NO₂ and O₃ at soil and leaf surfaces in an Amazonian rain forest, *J. Geophys. Res.*, 107, 27.1–27.15, 2002a.
- Gut, A., van Dijk, S., Scheibe, M., Rummel, U., Welling, M., Ammann, C., Meixner, F., Kirkman, G., Andreae, M., and Lehmann, B.: NO emission from an Amazonian rain forest soil: Continuous measurements of NO flux and soil concentration, *J. Geophys. Res.*, 102, 24.1–24.10, 2002b.
- Hanson, D. T. and Sharkey, T. D.: Effect of growth conditions on isoprene emission and other thermotolerance-enhancing compounds, *Plant, Cell Env.*, 24, 929–936, 2001a.
- Hanson, D. T. and Sharkey, T. D.: Rate of acclimation of the capacity for isoprene emission in response to light and temperature, *Plant, Cell Env.*, 24, 937–946, 2001b.
- Harley, P., Litvak, M., Sharkey, T. D., and Monson, R.: Isoprene emission from velvet bean leaves. Interactions among nitrogen availability, growth photon flux density, and leaf development, *Plant Physiology*, 105, 279–285, 1994.
- Harley, P., Vasconcellos, P., Vierling, L., Pinheiros, C. C. d. S., Greenberg, J., Guenther, A., Klinger, L., Almeida, S. d., Neill, D., Baker, T., Philipps, O., and Malhi, Y.: Variation in potential for isoprene emissions among Neotropical forest sites, *Global Change Biol.*, 10, 1–21, 2004.
- Holzinger, R., Lee, A., Paw U, K. T., Goldstein, A.: Observations of oxidation products above a forest imply biogenic emissions of very reactive compounds, *Atmos. Chem. Phys.*, 5, 67–75, 2005, **SRref-ID: 1680-7324/acp/2005-5-67**.
- Jacob, D. and Wofsy, S.: Budgets of Reactive Nitrogen, Hydrocarbons, and Ozone Over the Amazon Forest during the Wet Season, *J. Geophys. Res.*, 95, 16 737–16 754, 1990.
- Jacobs, A., Van Boxel, J., and El-Kilani, R.: Nighttime free convection characteristics within a plant canopy, *Bound.-Layer Meteorol.*, 71, 375–391, 1994.
- Kesselmeier, J., Kuhn, U., Rottenberger, S., Biesenthal, T., Wolf, A., Schebeske, G., Andreae, M., Ciccioli, P., Brancaleoni, E., Frattoni, M., Oliva, S., Botelho, M., Silva, C., and Tavares, T.: Concentrations and species composition of atmospheric volatile organic compounds (VOC) as observed during wet and dry season in Rondonia (Amazonia), *J. Geophys. Res.*, 107, 20.1–20.13, 2002.
- Kruijt, B., Malhi, Y., Lloyd, J., Nobre, A., Miranda, A., Pereira, M., Culf, A., and Grace, J.: Turbulence statistics above and within two Amazon rain forest canopies, *Bound.-Layer Meteorol.*, 94, 297–331, 2000.
- Kuhn, U., Rottenberger, S., Biesenthal, T., Wolf, A., Schebeske, G., Ciccioli, P., Brancaleoni, E., Frattoni, M., Tavares, T., and Kesselmeier, J.: Seasonal differences in isoprene and light-dependent monoterpene emission by Amazonian tree species, *Global Change Biol.*, 10, 663–682, 2004.
- Kurpius, M., Goldstein, A.: Gas-phase chemistry dominates O₃ loss to a forest, implying a source of aerosols and hydroxyl radicals to the atmosphere, *Geophys. Res. Lett.*, 30(7), 24.1–4, 2003.
- Leuning, R., Kelliher, F. M., de Pury, D. G. G., and Schulze, E. D.: Leaf nitrogen, photosynthesis, conductance and transpiration: scaling from leaves to canopies, *Plant, Cell Env.*, 18, 1183–1200, 1995.
- Lloyd, J., Grace, J., Miranda, A. C., Meir, P., Wong, S. C., Miranda, B. S., Wright, I. R., Gash, J. H. C., and McIntyre, J.: A simple calibrated model of amazon rainforest productivity based on leaf biochemical properties, *Plant, Cell Env.*, 18, 1129–1145, 1995a.
- Lloyd, J., Wong, S. C., Styles Julie, M., Batten, D., Priddle, R., Turnbull, C., and McConchie, C. A.: Measuring and modelling whole-tree gas exchange, *Aust. J. Plant Physiol.*, 22, 987–1000, 1995b.
- Mahrt, L.: Stratified atmospheric boundary layers, *Bound.-Layer Meteorol.*, 90, 375–396, 1999.
- Malhi, Y., Nobre, A. D., Grace, J., Kruijt, B., Pereira, M. G. P., Culf, A., and Scott, S.: Carbon dioxide transfer over a Central Amazonian rain forest, *J. Geophys. Res.*, 103, 31 593–31 612, 1998.
- Malhi, Y., Pegoraro, E., Nobre, A. D., Pereira, M. G. P., Grace, J., Culf, A., Clement, R.: Energy and water dynamics of a central Amazonian rain forest. *J. Geophys. Res.*, 107(D20), 45.1–45.17, 2002.
- Massman, W.: A review of the molecular diffusivities of H₂O, CO₂, CO, O₃, SO₂, NH₃, N₂O, NO and NO₂ in air, O₂ and N₂ near STP, *Atmos. Environ.*, 32, 1111–1127, 1998.
- McWilliam, A.-L., Roberts, J., Cabral, O., Leitao, M., Costa, A. d., Maitelli, G., and Zamparoni, C.: Leaf area index and above-ground biomass of terra firme rain forest and adjacent clearings in Amazonia, *Funct. Ecol.*, 7, 310–317, 1993.
- Meixner, F., Ammann, C., Rummel, R., Gut, A., and Meinrat, O.: The rain forest canopy reduction effect on NO emission from soils, in: 10th Scientific Conference of the International Association of Meteorology of Atmospheric Sciences (IAMAS) Commission for Atmospheric Chemistry and Global Pollution (CACGP) and 7th Scientific Conference of the International Global Atmospheric Chemistry Project (IGAC), Crete, Greece, 2002.
- Moore, C. and Fisch, G. F.: Estimating heat storage in Amazonian tropical forest, *Agric. For. Meteorol.*, 38, 147–169, 1986.
- Neubert, A., Kley, D., and Wildt, J.: Uptake of NO, NO₂ and O₃ by sunflower (*Helianthus annuus* L.) and tobacco plants (*Nico-*

- tiana tabacum* L.): dependence on stomatal conductivity, Atmos. Environ., 27, 2137–2145, 1993.
- Padro, J., Neumann, H., and den Hartog, G.: Modelled and observed dry deposition velocity of O₃ above a deciduous forest in the winter, Atmos. Environ., 26A, 775–784, 1992.
- Raupach, M. R.: Applying Lagrangian fluid mechanics to infer scalar source distributions from concentration, Agric. For. Meteorol., 47, 85–108, 1989.
- Reich, P., Uhl, C., Walters, M., and Ellsworth, D.: Leaf lifespan as a determinant of leaf structure and function among 23 Amazonian tree species, Oecologia, 86, 16–24, 1991.
- Rinne, H., Guenther, A., Greenberg, J., and Harley, P.: Isoprene and monoterpenes fluxes measured above Amazonian rainforest and their dependence on light and temperature, Atmos. Environ., 36(14), 2421–2426, 2002.
- Roberts, J., Cabral Osvaldo, M. R., Fisch, G., Molion, L. C. B., Moore, C. J., and Shuttleworth, W. J.: Transpiration from an Amazonian rainforest calculated from stomatal conductance measurements, Agric. For. Meteorol., 65, 175–196, 1993.
- Rummel, U.: Turbulent exchange of ozone and nitrogen oxides from a tropical rain forest in Amazonia, Phd thesis, University Bayreuth, Germany, 2005.
- Sellers, P., Berry, J., Collatz, G., Field, C., and Hall, F.: Canopy reflectance, photosynthesis and transpiration. III: A reanalysis using improved leaf models and a new canopy integration scheme, Remote Sens. Environ., 42, 187–216, 1992.
- Sharkey, T. D., Loreto, F., and Delwiche, C.: High carbon dioxide and sun/shade effects on isoprene emission from oak and aspen tree leaves, Plant, Cell Env., 14, 333–338, 1991.
- Simon, E., Meixner, F., Ganzeveld, L., and Kesselmeier, J.: Coupled carbon-water exchange of the Amazon rain forest, I. Model description, parameterization and sensitivity analysis, Biogeosciences, 2, 231–251, 2005a, **SRef-ID: 1726-4189/bg/2005-2-231**.
- Simon, E., Lehmann, B., Ammann, C., Ganzeveld, L., Rummel, U., Nobre, A., Araujo, A., Meixner, F., Kesselmeier, J.: Lagrangian dispersion of ²²²Rn, H₂O and CO₂ within Amazon rain forest, Agric. For. Meteorol., in press, 2005b.
- Staudt, M., Joffre, R., and Rambal, S.: How growth conditions affect the capacity of *Quercus Ilex* leaves to emit monoterpenes, New Phytol., 158, 61–73, 2003.
- Stefani, P. R., Valentini, R., and Ciccioli, P.: Preliminary assessment of VOC fluxes from a primary rainforest performed at the LBA site at Manaus, in: Proceedings of the First LBA Scientific Conference, edited by: Artaxo, P. and Keller, M., MCT, Belem, Brazil, 2000.
- Stull, R. B.: An Introduction to Boundary Layer Meteorology, Atmospheric Science Library, Kluwer Academic Publishers, Dordrecht, 1988.
- Wesely, M.: Parameterization of surface resistance to gaseous dry deposition in regional-scale numerical models, Atmos. Environ., 23, 1293–1304, 1989.
- Wesely, M. and Hicks, B.: A review of the current status of knowledge on dry deposition, Atmos. Environ., 34, 2261–2282, 2000.
- Wesely, M., Sisterson, D., and Jastrow, J.: Observations of the chemical properties of dew on vegetation that affect the dry deposition of SO₂, J. Geophys. Res., 95, 7501–7514, 1990.
- Williams, M., Malhi, Y., Nobre, A. D., Rastetter, E. B., Grace, J., and Pereira, M. G. P.: Seasonal variation in net carbon exchange and evapotranspiration in a Brazilian rain forest: a modelling analysis, Plant, Cell Env., 21, 953–968, 1998.
- Yienger, J. and Levy, H. I.: Empirical model of global soil-biogenic NO_x emissions, J. Geophys. Res., 100, 11 447–11 464, 1995.
- Zimmerman, P., Greenberg, J., and Westberg, C.: Measurements of atmospheric hydrocarbons and biogenic emission fluxes in the Amazon boundary-layer, J. Geophys. Res., 93, 1407–1416, 1988.